The anticancer effects induced by the bacterial protein azurin: evaluation of cytotoxicity, membrane destabilization and cell death in multiple cancer cell models

Luís Filipe Xavier Rodrigues Coutinho

Dissertation to obtain the Master of Science Degree in

Biomedical Engineering

Supervisors:

Professor Faustino Mollinedo

Professor Arsénio do Carmo Sales Mendes Fialho

Examination Committee

Chairperson: Professor Maria Margarida Fonseca Rodrigues Diogo

Supervisor: Professor Arsénio do Carmo Sales Mendes Fialho

Member of the Committee: Doctor Karina Marangoni

July 2021

If we knew what it was we were doing, it would not be called research, would it?
Albert Einstein

Research is seeing what everybody else has seen and thinking what nobody else has thought.
Albert Szent-Györgyi

As for the future, your task is not to foresee it, but to enable it.
Antoine de Saint Exupery

Preface

The work presented in this thesis was performed at the Center for Biological Research (CIB, Madrid, Spain) of the Spanish National Research Council (CSIC, Spain), during the period October 2019-February 2020, under the supervision of Prof. Faustino Mollinedo. The thesis was co-supervised at Instituto Superior Técnico by Prof. Arsénio Fialho.

Declaration

I declare that this document is an original work of my own authorship and that it fulfils all the requirements of the Code of Conduct and Good Practices of the Universidade de Lisboa.

Acknowledgments

First and foremost, to my parents and sister to whom words of thanks would never suffice, neither will I ever be able to properly convey how appreciative I am, for the curiosity about the inner workings of world you instilled on me, the encouragement and unfathomable patience, but beyond all, the tenacity, perseverance and the support in those dark dark sleepless nights and agonizing days. Parents should never have to go through that and I would definitely not be here if it were not for you.

I thank my family who always believed in me and helped whenever possible. Special remarks go to my grandfathers Florêncio and Manuel who above anyone cultivated my interests in science and engineering, and were most excited by me enrolling in an engineering MSc. Unfortunately, they were not able to witness its conclusion but forever will be in my memory.

I thank to my true friends for never giving up on me and never letting me give up. All the emotional support has been very much appreciated.

I warmly thank my supervisor Prof. Faustino Mollinedo and the associates of the Laboratory of Cell Death and Cancer Therapy, Consuelo Gajate, Julia Mayor and Alba Vicente-Blázquez, for welcoming me into their research group and the support, knowledge and the advice they altruistically provided.

I am also extremely thankful to Nuno Bernardes for the guidance provided and the availability to produce and purify the azurin used in the experiments performed for this thesis.

I am sincerely grateful to Professor Arsénio Fialho for the chance to do my experimental work in such a renowned international institution, the godly amount of patient and care, the advice and knowledge, but above all the dedication and opportunities given to me over the years for which I forever will be in his debt.

Finally, I thank you all, from inspiring teachers to caring individuals, who somehow directly or indirectly contributed to make this thesis possible.

Abstract

Azurin is a protein secreted by the bacterium *Pseudomonas aeruginosa* which has been studied as an anticancer agent. This exploratory work aims to contribute to the elucidation of the extent of cell proliferation inhibition, membrane disruption and cell death in multiple cancer cell lines (HeLa, cervix adenocarcinoma; AGS, gastric adenocarcinoma; and U2OS, osteosarcoma) upon treatment with azurin. In order to ascertain cell proliferation MTT assays were performed. To measure membrane disruption and cell death PI-FL3 flow cytometry was employed (with non-fixed and fixed cells, respectively). After 72 h exposure to treatment (100 µM azurin), all cancer cell lines showed a dose dependent proliferation inhibition regardless of p53 status with IC_{50} roughly estimated to be around 140 µM for HeLa, 75 µM for AGS and 70 µM for U2OS. Azurin contributed to the destabilization of the cell membrane upon long exposures (72 h) with 16.4±6.4% (HeLa), 45.9±5.0% (AGS), 19.9±10.6% (U2OS) and 10.3%[1] (BHK, non-tumorigenic fibroblast cell line) propidium iodide (PI) permeable populations. This destabilisation was superior relative to the observed cell death, with HeLa, AGS, U2OS cells presenting 6.9±3.2%, 14.9±4.6%, 6.8±3.9% hypoploid populations, respectively, (corresponding to dead cells with fragmented DNA) upon treatment with 100 µM at 72 h of azurin WT against the 4.6±0.8% hypoploid population in BHK cells. Thus, in this work it was observed that azurin has an anti-proliferative (cytostatic) effect in the tested cell lines with apparent membrane disruption in the population. Although present, azurin appears to have limited cytotoxic effects by itself and, given its diffuse mode of action, it seems more reasonable to use azurin as a co-adjuvant with a synergistic effect, in order to enhance the efficacy of other anti-cancer drugs and possibly to surpass multidrug resistance events, rather than as a standalone therapeutic.

Key words: Azurin, anti-cancer therapies, cell death, membrane destabilization.

[1] BHK treated with azurin F114A had no replicas, thus data were statistically invalid.

Resumo

A azurina é uma proteína excretada pela bactéria *Pseudomonas aeruginosa* que tem vindo a ser estudada como um agente anticancerígeno. Este trabalho exploratório visa contribuir para a elucidação da extensão da inibição da proliferação celular, disrupção da membrana, e morte celular em múltiplas linhas celulares cancerígenas (HeLa, adenocarcinoma da cérvix; AGS, adenocarcinoma do estômago; e U2OS, osteossarcoma), após tratamento com azurina. Foram realizados ensaios de MTT para determinar a proliferação celular, e citometria de fluxo IP-FL3 para medir a disrupção da membrana e a morte celular (células não fixas e fixas, respetivamente). Após exposição a 72 h de tratamento (100 µM de azurina) todas as linhas cancerígenas testadas apresentaram inibição dose-resposta na proliferação independentemente do p53 *status*, com uma estimativa aproximada para os IC_{50} de 140 µM para HeLa, 75 µM para AGS e 70 µM for U2OS. A azurina contribuiu para a desestabilização da membrana celular para exposições de longa duração (72 h) com 16.4±6.4% (HeLa), 45.9±5.0% (AGS), 19.9±10.6% (U2OS) e 10.3%[1] (BHK, linha celular não tumoral de fibroblasto) das populações permeáveis a iodeto de propídio (IP). Esta desestabilização foi superior à morte celular, onde HeLa, AGS e U2OS apresentaram 6.9±3.2%, 14.9±4.6% e 6.8±3.9% da população hipoploide (que corresponde a células mortas com ADN fragmentado) após tratamento com azurina a 100 µM durante 72 h, comparativamente aos 4.6±0.8% observados para BHK. Neste trabalho observou-se que a azurina tem um efeito antiproliferativo (citostático) nas linhas celulares testadas, com aparente disrupção da membrana ao nível populacional. Embora presente, a azurina aparenta, por si só, ter efeitos citotóxicos limitados, e dado o seu modo de ação difuso, parece mais razoável o uso da azurina como coadjuvante com efeito sinergístico, com o intuito de melhorar a eficácia de outros fármacos anticancerígenos e possivelmente para mitigar eventos de indução de multirresistência, em vez da sua utilização individual.

Palavras-chave: Azurina, terapias anticancerígenas, morte celular, desestabilização membranar.

Table of Contents

List of Tables

List of Figures

List of Abbreviations

3D – Three dimensions/ Three-dimensional

AGS – Human gastric adenocarcinoma, ATCC CRL-1739

ATCC – American Type Culture Collection

ATP – Adenosine triphosphate

BHK/BHK-21 – Baby Hamster Kidney fibroblast, ATCC CCL-10

***cf.* –** from Latin *'confer'*, «confer»

DMEM – Dulbecco's Modified Eagle Medium

DMEM/F12 – Dulbecco's Modified Eagle Medium supplemented with Ham's Nutrient Mixture F12

e.g. – from Latin *'exempli gratia'*, «for example»

FBS – Fetal Bovine Serum

HeLa – Human cervix adenocarcinoma, ATCC CCL-2

IC $_x$ – x% maximal inhibitory concentration

***i.e.* –** from Latin *'id est'*, «this is»

IL – Interleukin

i.p. – Intraperitoneal injection

i.v. – Intravenous injection

IPTG – IsoPropyl-β-D-ThioGalactopyranoside

K_d – Dissociation constant

LB medium – Luria Broth medium

MTT – 3-(4,5-dimethylthiazol-2-yl)-2,5-diphenyl tetrazolium bromide

Mut – Mutant

p53 – Cellular Tumor Antigen p53 (UniProt name)

PI – Propidium Iodide

PI-FL3 flow cytometry – Propidium Iodide flow cytometry detected on the FL3 channel (620/30 nm)

PBS – Phosphate Buffered Saline

PDB – Protein Data Bank

s.c. injection – Subcutaneous injection

SD – Standard Deviation

SEM – Standard Error of the Mean

SB medium – Super Broth medium

U2OS – Human osteosarcoma, ATCC HTB-96

WT – Wild-Type

Membrane fouling index

Non-SI Units:

CFU/g – colony-forming unit per gram

Da – Dalton/ Unified atomic mass unit

MFI – Membrane fouling index

rpm – Revolution per Minute

% – Percent

ºC – Degree Celsius

1 Introduction

1.1 Cancer

Cancer, also commonly named neoplasm or malignant tumour, is a group of diseases characterized as the uncontrolled growth/multiplication of abnormal cells from any organ or tissue of the body with the ability to metastasize, *i.e.* go beyond their usual anatomo-physiological boundaries to invade and spread to adjoining tissues and/or other organs in the body [1].

According to the Global Burden of Disease Study 2017 findings, cancer is the second most common human cause of death, both in the developed and developing countries, and a major health problem worldwide [2]. The status report on the global burden of cancer worldwide, based on GLOBOCAN 2018 estimates of cancer incidence and mortality, produced by the International Agency for Research on Cancer, states that there were an estimated 18.1 million new cancer cases and 9.6 million cancer deaths (about 16% of the total number of deaths). The most prevalent cancers were lung cancer (11.6% of the total cases), female breast cancer (11.6%), colorectum cancer (10.2%) and prostate cancer (7.1%). Regarding mortality, in males, lung cancer lead in fatalities (22.0% of cancer deaths), followed by liver cancer (10.2%), stomach cancer (9.5%), colorectum cancer (9.0%) and prostate cancer (6.7%). Amongst females, breast cancer is the most commonly diagnosed and the leading cause for cancer death (15.0%), followed by lung cancer (13.8%), colorectum cancer (9.5%), cervix cancer (7.5%) and stomach cancer (6.5%) [[3], [4]].

The collaborators of the Global Burden of Disease Study 2015 Risk Factors found that tobacco use (cigarette smoking) is the most relevant risk factor for cancer, by being responsible for approximately 22% of cancer deaths. Other risk factors for cancer are unhealthy dietary habits, alcohol and drug abuse, occupational hazards and, predominantly for women, unsafe sex due to human papilloma virus (HPV) infection [5]. Furthermore, infections that might lead to cancer, such as Helicobacter pylori, Human HPV, Hepatitis B virus, Hepatitis C virus, and Epstein-Barr virus, are responsible for up to 25% of cancer cases in low- and middle-income countries [1].

Cancer arises from the gradual transformation of normal cells into tumour cells in a multistage process. Generally, it progresses from a pre-cancerous lesion to a malignant tumour, as the result of interactions between the individual's genetic factors and the scope of exposure to carcinogens [1]. Carcinogens are external agents that upon interaction with the body directly promote or support cancer onset and/or progression, usually through DNA damage. These gene mutations lead to overexpression of oncogenes or the inhibition of tumour suppressor genes, which unbalances the cell proliferation control towards uncontrolled and ungated cell division [6].

There are three broadly categorizable carcinogen groups: chemical, physical and biological carcinogens. Chemical carcinogens include agents such as the above mentioned tobacco smoke components, asbestos, arsenic (a drinking water contaminant) and aflatoxin (a food contaminant); physical carcinogens include ultraviolet and ionizing radiation and biological carcinogens comprise of certain infectious viruses, bacteria, or parasites [1].

Conventional therapies mainly attempt to treat the disease by surgical resection, radiotherapy, and chemotherapy. However, tumour polymorphism and development of drug chemoresistance, as well as off target and treatment-related side effects, limit the efficacy of many therapeutic options as the disease progresses [7]. Significant advances have been made in the last two decades, with the development and clinical approval of targeted therapeutics such as receptor tyrosine kinase inhibitors (e.g., erlotinib in 2003) [8] and immunotherapy with personalized cancer vaccines (e.g., pembrolizumab in 2014) [9]. These compounds present much higher selectivity for cancer cells with minimum side effects compared with conventional treatment. Unfortunately, despite the efforts, many malignancies remain impossible to treat with these approaches.

1.2 Properties of Azurin and derived peptides

1.2.1 Structure and amino acid sequences

Azurin (**Figure 1**) is a low molecular weight redox protein from the opportunistic pathogenic bacteria *Pseudomonas aeruginosa.* It belongs to the cupredoxin superfamily, which encompasses small water-soluble copper-containing proteins (10–20 kDa) involved in electron transfer reactions. This protein consists of 128 amino acids and has about 14 kDa of molecular weight. Other azurins can be found in some members of the gamma and beta subdivisions of the Proteobacteria, but they are absent from all other bacterial phyla and the Eukarya. Although the sequence homology between the azurins varies between 50 and 90%, the structural homology between these molecules is highly conserved. All azurins present a characteristic single-domain signature consisting of a compact structurally rigid β-sandwich core, the immunoglobulin fold, formed by two main β-sheets made up of seven or more parallel and anti-parallel strands (β-barrel structure) and also possess an essentially neutral hydrophobic patch surrounding the copper site [[10], [11]].

The hydrophobic patch provides a stable framework structure in the presence of disulphides enabling thermal stability retention even when its surface loops are replaced, thus opening azurin as an alternative protein scaffold. Moreover, given the immunoglobulin (Ig)-like domain with loops at the two poles, this protein is non-immunogenic and allows for a large binding interface [12].

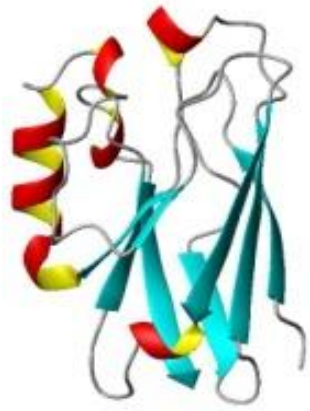

Figure 1 3D structure of Azurin from *Pseudomonas aeruginosa*. PDB ID: 1jzg

Azurin from *Pseudomonas aeruginosa* can be readily overexpressed in *E. coli* and purified (*cf.* Materials and methods), however it is difficult to ensure proper endotoxin removal. Thus, it is a challenge to maintain economical sustainability while following the Food and Drug Administration (FDA) and the European Medicines Agency (EMA) specifications for commercial use in humans. Therefore, continuous efforts have been made in order to isolate specific peptide sequences with high potential in anti-cancer applications. These anticancer peptides (ACPs) candidates can be readily chemically synthesized, completely solving the endotoxin removal concern. The most well studied azurin derived peptides are p28 and p18; however, new peptides are being developed, studied and tested such as CT-p19LC.

p28 is an azurin derived peptide consisting of the Leu50-Asp77 protein fragment. It encompasses a β-strand, an α-helix, a turn, and an irregular structure (**Figure 2**). Although, p28 is folded into a stable three-dimensional structure within azurin, it does not mean that the p28 fragment forms the same structure as an isolated peptide. In fact, molecular dynamics simulations showed that the α-helix of p28 is unstable after isolation [[12], [13]]. p18 is the minimal motif for the protein transduction domain (PTD) of azurin which encompass the first 18 amino acids of p28 [14]. CT-p19LC is a 19-residue optimized peptide derived from CT-p26, another 26-residue peptide derived from the 94-120 amino acids of azurin [15].

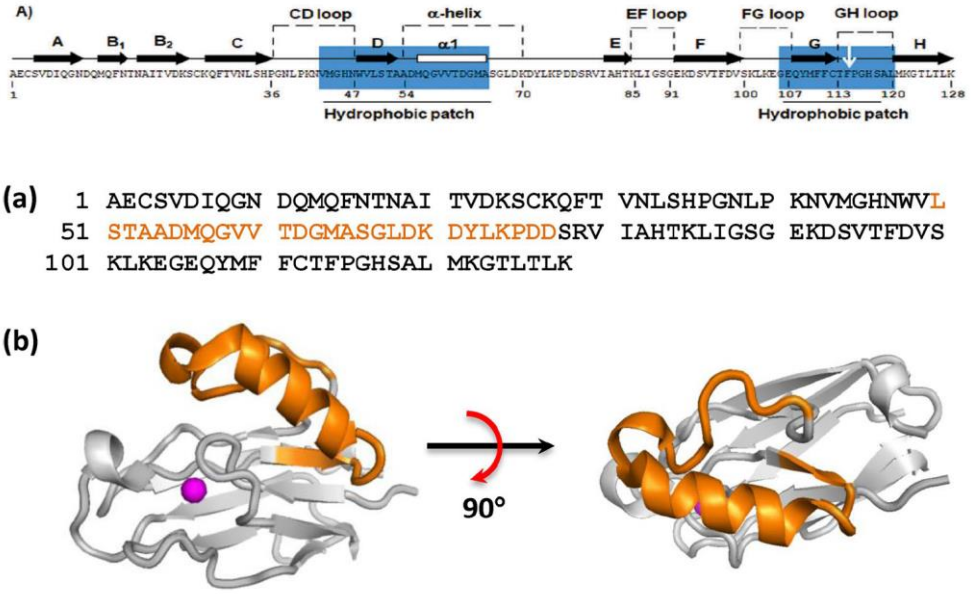

Figure 2 Amino acid sequences and three-dimensional structures of azurin and p28. a) Amino acid sequence of azurin. The region corresponding to p28 is shown in orange and hydrophobic patch in blue. b) Three-dimensional structure of azurin (PDB ID 2xv2). The region corresponding to p28 is shown in orange. The copper ion is shown as a purple sphere (extracted from [16]).

1.2.2 Preferential Entry into Cancer Cells

Azurin preferentially enters a variety of human cancer cells while it is inefficiently internalized in normal cells. For instance, UISO-Mel-2 melanoma cells and MCF-7 breast cancer cells readily

internalize the protein for 1 to 6 h of incubation time with azurin (7 μM), while normal peritoneal macrophages**,** mast cells and MCF-10F cells hardly took it up [17].

Truncation experiments reveal that penetration through the cell membrane is mediated mainly by the p28 region (amino acids 50–77). Moreover, p28 (3 kDa) can promote payload internalization of 53 kDa cargo proteins in macrophages and melanoma cells. Since the p28, glutathione S-transferase and green fluorescent protein fusion construct (NH_2–GST–GFP–p28–COOH, 7 μM, 1 h incubation) is internalized by J774 and UISO-Mel-2 cells, whilst the GST–GFP fusion protein (7 μM, 1 h incubation) alone was retained at the surface (confocal microscopy analysis) [17]. Competition assays found that azurin increasingly competes with labelled GST–p28 for entry into UISO-Mel-2 cells in a dose dependent manner, thus demonstrating that a common receptor is responsible for binding and internalization of azurin and p28 [17].

The Yamada *et al.* (2005) studies showed that J774 cells present 40% less GST–GFP–p28 (1.8 μM, 1 h) penetration after incubation with Protonophore carbonyl cyanide m-chlorophenylhydrazone[2] (CCCP; 10 μM, 1 h), analysed by fluorescence-activated cell sorting (FACS). In addition, UISO-Mel-2 showed inhibition of Alexa fluor 568-conjugated azurin (14 mM) internalization after incubation with CCCP (20 μM) or cytochalasin D[3] (0.5 μM), while not showing inhibition in internalization after incubation with Brefeldin A[4] (BFA; 18 μM), observed through confocal microscopy. This observation suggests that azurin internalization is mediated, at least in part, by a receptor-mediated endocytic process [17].

Taylor *et al.* (2009) assays with inhibitors point that energy-dependent (*i.e.* ATP-dependent) transport mechanisms, clathrin mediated endocytosis or micropinocytosis and microtubule stabilization seem not to be involved in p28 cell penetration, while membrane micro domains (*i.e.*, Lipid rafts), caveolae-mediated endocytosis and the Golgi complex are of great importance in p28 and azurin cell penetration. Since sodium azide[5] (1 mM; 60 min), ouabain[6] (50 mM; 60 min), chlorpromazine[7] (CPZ; 10 μg/mL; 60 min), amiloride[8] (50 μM; 30 min) and Taxol[9] (20 μM; 30 min) had no effect in p28 (Alexa Fluor 568–labelled p28, 20 μM; 1 h) penetration into UISO-Mel-2 cells, but nocodazole[10] (10 μmol/L; 60 min; 50-65% inhibition), monensin[11] (10 μM; 60 min; 50% inhibition), BFA (100 μM; 60 min; 30% inhibition), methly-β-cyclodextrin[12] (MβCD; 5 mM; 60 min; 60% inhibition); filipin[13] (3 μg/mL; 60 min;

[2] Protonophore carbonyl cyanide m-chlorophenylhydrazone (CCCP) is a mitochondrial uncoupler of energy generation.

[3] Cytochalasin D is a known inhibitor of receptor-mediated endocytosis that disrupts the cellular microfilament network.

[4] Brefeldin A (BFA) is known to disrupt the Golgi apparatus and inhibit classical vesicle-mediated secretion.

[5] Sodium azide is a metabolic inhibitor.

[6] Ouabain is a specific inhibitor for the sodium-potassium ion pump (Na/K-ATPase).

[7] Chlorpromazine (CPZ) is a clathrin-mediated endocytosis inhibitor.

[8] Amiloride is macropinocytosis inhibitor.

[9] Taxol is a microtubule stabilizer.

[10] Nocodazole inhibits caveosome formation.

[11] Monensin inhibits at late endosome/lysosome.

[12] Methly-β-cyclodextrin (MβCD) is a cholesterol depletion agent extracting it from the cell's membrane outer leaflet continuously.

[13] Filipin and nystatin are polyene macrolide antibiotics that exhibit potent antifungal activity. In cellular biology they are used as inhibitors of the raft/caveolae endocytosis pathway on mammalian cells (at concentrations around 3 μg/mL);

35% inhibition), nystatin (50 µg/mL; 30 min; 50% inhibition) and tunicamycin[14] (20 µg/mL; 48 h; 55% inhibition) did inhibited the penetration of p28 in the UISO-Mel-2 cells, using flow cytometric analysis. The penetration of p28 is also inhibited in non-cancerous fibroblasts by MβCD, nocodazole, monensin, and tunicamycin, but not by amiloride, sodium azide, and CPZ [14]. Similarly, MCF-7 cells are more sensitive to the effects of MβCD (~2.1-fold higher), filipin (~1.2-fold higher), and nocodazole (~1.6-fold higher) than MCF-10A normal cells. But yet again, peptide penetration is inhibited by MβCD, filipin and nocodazole but not by amiloride, chlorpromazine, and sodium azide in both cell lines [18]. Thus, at least one mechanism of entry into cancer and normal cells may be similar, but preferential accumulation into cancer cells may be a function of the number of common membrane receptors or structures, *i.e.*, caveolae [14]. However, it is noteworthy that p28 fluorescence is 0.5 to 6-fold higher in cancer cell lines (UISO-Mel2, melanoma; DU145, prostate cancer; SKOV-3, ovarian cancer; A549, lung cancer; MFC-7, breast cancer) as compared to the corresponding normal counterparts (normal fibroblasts; CRL11611, normal prostate; HOSE6-3, normal ovarian; CCD13-Lu, normal lung; MCF-10A, normal breast) through FACS analysis. Moreover, cell penetration by azurin, p28 and p18 does not result from membrane disruption at least for a 10 min exposure at 37 °C, and up to 100 µM there was no difference to the control in a LDH leakage assay of UISO-Mel-2 [14].

p28 penetration in MCF-7 cells (V_{max}, 1.89 MFI/s; K_m, 144.3 µM) and in MCF-10A cells (V_{max}, 0.79 MFI/s; K_m, 99.4 µM) is saturable, ~2.4-fold faster in MCF-7 compared with MCF-10A [18]. However, in UISO-Mel-2 (V_{max}, 1.87 MFI/s; K_m, 159.1 µM) and normal fibroblasts (V_{max}, 1.89 MFI/s; K_m, 166.0 µM) the peptide entry kinetics for normal and cancer cells is virtually identical, determined by FACS [14].

Although p28 is the main segment that mediates azurin cell penetration, hydrophobic residues adjacent to the p28 segment in space may also be involved [16]. Bernardes *et al.* (2018) studied the role of the hydrophobic patch surrounding the copper site in the interaction of azurin with the lipid raft components ganglioside GM-1 and caveolin-1 in the cell membrane, given the previous notions of azurin's co-localization and caveolae-mediated endocytosis in cancer cells. Through a point mutation from the aromatic residue Phe114 to alanine, it was observed a reduction in cell penetration in MCF-7 breast cancer, HeLa cervix cancer and HT-29 colon cancer cells, respectively, 20±2%, 15±1% and 62±5% for a 2h incubation period with 50 µM azurin F114A *versus* the wild-type (WT) counterpart, and 32±3%, 47±7% and 53±4% for 100 µM [19]. It is noteworthy that these findings were produced through cell lysate Western Blots, therefore only reflect the internalization of azurin in intact cells at the time of harvesting. CAV1 silencing siRNA assays in MCF-7 and HeLa found that a 35±7% and 58±4% reduction in Caveolin-1 expression, respectively, produced a 58±3% and 18±3% decrease in WT azurin internalization. For similar silencing the mutated protein uptake was unchanged. Also, blocking GM-1 ganglioside with Cholera Toxin B subunit[15] (CTxB; 1µg/mL; 10min) reduces the penetration of azurin (50 µM; 30 min) by 48±6% for WT and 60±7% for F114A, both in MCF-7 and HT-29, *i.e.* blocking GM-1 ganglioside with CTxB reduce azurin uptake by cancer cells by about a half,

[14] Tunicamycin is an N-linked glycosylation inhibitor;

[15] Cholera Toxin B subunit (CTxB) is a component of a heat-labile enterotoxin produced by Vibrio cholerae, is a probe commonly used to label and/or detect GM1 ganglioside which can be used as marker for lipid rafts, since the GM-1 ganglioside has an abundant localization in these membrane microdomains, for this application it is used as a bloker.

independently of the presence of the hydrophobic patch; Although, the authors point that a change in membrane raft morphology, due to lipid-raft crosslinking by CTxB, is not possible to rule-out as a cause for this result [19].

1.2.3 Effects in cancer cell metabolism

Azurin is a versatile protein that interferes in several independent signalling pathways associated with cancer progression, such as the p53 and receptor tyrosine kinase pathways [20] and presents extracellular effects such as modulation of cell membrane properties and supress tumour angiogenesis [21]. It has been suggested that this protein presents this promiscuous behaviour due to its low binding affinity for its targets allowing it to have the potential to become new anticancer drug not easily susceptible to induce cancer resistance [22].

Stabilization of p53 Protein

It has been demonstrated that azurin can directly interact and stabilize the tumour suppressor p53 [20]. Complex formation between WT azurin and p53 is detected in various glycerol gradient centrifugation fractions by Western blotting with anti-azurin and anti-p53 monoclonal antibodies. This interaction seems to be specific given that all controls with glutathione (GST), ovalbumin and E3 ubiquitin-protein ligase Mouse double minute 2 homolog binding domain (MDM2-BD) did not present complex formation with azurin [23]. It also points that azurin interaction and stabilization of p53 is independent from the oncogene Mdm2 pathway, which is the main p53 down-regulator. However it is possible that the 4 kDa size of the MDM2-BD is just not heavy enough to allow for MDM2-BD/azurin complexes to be detected in fractions besides the natural one for non-complexed azurin.

Stabilization of p53 is observed in UISO-Mel-2 cells incubated for 12 h with buffer (control), followed by the addition of cycloheximide to prevent protein synthesis. The level of p53 after 2 h sharply declines to near zero while ~50% of the original p53 remains for azurin treated cells (36 µM) by Western blotting using anti-p53 monoclonal antibodies [23]. Furthermore, azurin treatment (36 µM; 12 h) increases substantially the level of intracellular p53 in the cytosolic, nuclear fractions and slightly increases its level in the mitochondria. In addition, confocal microscopy comparison of UISO-Mel-2 ($p53^+$) with UISO-Mel-6 ($p53^-$) after azurin treatment found that p53 performs a relevant role in the transport of azurin to the nucleus [23].

In human breast cancer, p53 expression increases and reaches its maximum after 24 h for MCF-7 cells ($p53^+$) treated with azurin (56 µM). p53-dependent modulation unbalances in Bcl-2-associated X protein (Bax) and B-cell lymphoma 2 (Bcl2) gene expression appear to be present given the 3-fold Bax/Bcl2 observed at 24 h in comparison with the control. Translocation of cytochrome *c* from the mitochondria to the cytosol is also observed, pointing that azurin may induce apoptosis in MCF-7 cells through p53 stabilization and the induction of the intrinsic apoptotic pathway [24]. Note that for MDA-MB-157 (p53-null) and MDD2 and MDA-MB-231 cells (non-functional p53) there is a far less unbalance in *bax* and *bcl2* gene expression and there is no translocation of cytochrome *c* from the mitochondria to the cytosol [24]. Moreover, U2OS osteosarcoma cells ($p53^+$) show an ~4-fold increase in the Bax/Bcl2 ratio and a 5-fold increase in relative active caspase-3 when treated with azurin (14.3 µM; 24 h) in comparison with MG-63 cells [25].

Besides the direct effect interaction of azurin with p53, there is evidence that supports direct interaction between p28 and the aforementioned tumour suppressor. Following the bioinformatics and protein–protein interactions, using atomic force microscopy, between azurin and p53, studies by De Grandis *et al.* (2007) and Taranta *et al.* (2008, 2009), which supported the possibility for azurin to bind to the various domains of p53 in multiple configurations, similar molecular dynamic simulations (Santini *et al.* 2011) and atomic force spectroscopy experiments (Bizarri *et al.* 2011) demonstrated similar abilities for p28 [21].

The findings of GST pull-down assays suggest that p28 binds to p53, while, molar increases of p28 do not compete with GST–MDM2, pointing that any p28-induced decrease in the ubiquitination of p53 does not occur via a MDM2-mediated pathway. The MDM2-mediated pathway is the main p53 degradation pathway. Furthermore, the presence of p53 antibodies which recognize different motifs in the p53 protein (amino acids 32-79, 277-296, and 306-393) do not block p28 binding to p53. Thus p28 binds outside of these recognition sites, within a region bounded by either amino acids 1 to 18, 27 to 31, 80 to 276, or 297 to 305 [18]. This corroborates the *in silico* docking modelling supported by cluster analysis, molecular dynamics simulations and binding free energy calculations, which have model the interaction between the DNA-binding domain (DBD) of p53 and the p28 fragment and found that p28 is able to form a complex with the DBD characterized by favourable negative binding free energy, high shape complementarity, and the presence of several hydrogen bonds at the interface [12].

MCF-7 cells markedly increase the intracellular level of p53 upon exposure of p28 (50 μM) from ~2-fold after 24h up to ~3.3-fold at 72 h. Reverse transcription-Polymerase Chain Reaction (RT-PCR) experiments show that p53 transcription is not significantly altered after exposure to p28, suggesting that the increase in p53 occurred post-translationally [18]. In MCF-7 cells, the p53-specific high molecular weight ladder and smear bands resulting from p53 ubiquitination are reduced by 75%, 24 h and 50%, 48 h after treatment with p28 (50 μM). Note that the proteasome inhibitor MG132 was used to avoid p53-Ub_n degradation in order to ensure more accurate relative assessment of p53 ubiquitination [18].

The DNA-binding activity of p53 in nuclear extracts from MCF-7 cells treated with p28 (50 μM; 24h) or azurin (50 μM; 24h) are ~1.8- and ~2.3-fold higher than the untreated control. Subsequent elevation of the cyclin-dependent kinase inhibitors p21 (307%, 24h; 346%, 48 h; 271%, 72 h) and p27 (355%, 24h; 576%, 48 h; 926%, 72 h), CDK6 (138%, 24h; 178%, 48 h; 294%, 72 h) and cyclin B1 (393%, 24h; 633%, 48 h; 755%, 72 h); and reduction of cyclin-dependent kinase 2 (CDK2; 79.8%, 24h; 52.9%, 48 h; 57.9%, 72 h) and cyclin A (96.6%, 24h; 84.5%, 48 h; 77.1%, 72 h) levels in a time-dependent manner occurs in MCF-7 cells but not in MDD2 cells for which p53, cdc2, CDK2, CDK4, and CDK6 levels essentially remain constant [18].

Following these findings, *in silico* computational simulations were used to predict motifs within the p53–DBD as potential sites for p28 binding. Competitive pull-down GST–p53 assays results showed that GST–$p53_{1–393}$ (full length p53), GST–$p53_{81–300}$ (p53–DBD), GST–$p53_{81–160}$ and GST–$p53_{161–300}$ pulled down p28, but the N- (GST–$p53_{1–80}$) and C-terminus of p53 (GST–$p53_{301–393}$) and GST alone did not. Furthermore, the binding motifs of p28 and COP1 overlap, presented by

competitive pull-down assays of purified GST–p53 in the presence of excess p28. And, p28 induced a significant concentration-dependent reduction in the amount of the E3 ubiquitin ligase Fagol Caspase recruitment domain-containing protein 16 (COP1) binding to the p53–DBD. Fine mapping within the p53–DBD revealed that p28 inhibited COP1 binding only for GST–$p53_{81–300}$ and GST–$p53_{81–160}$, demonstrating that p28 inhibits the binding of COP1 only where their respective binding sites overlap [13].

In vitro direct studies, as well as, western blot and RT-PCR analyses determined that p28 decreases the level of COP1 more than 80% in $p53^{wt}$ (breast cancer, MCF-7; normal breast, MCF-10A; melanoma, UISO-Mel-29) and $p53^{mut}$ (breast cancer, MDA-MB-231; melanoma, UISO-Mel-23) cell lines, while no such decrease is observed in $p53^{dom/neg}$ (breast cancer, MDD2) or $p53^{null}$ (melanoma, UISO-Mel-6) cell lines.

Hence, p28 induces an increase in p53 levels through the formation of a p28:p53 complex which inhibits the binding of the COP1 to the p53 DNA-binding domains, thus preventing p53 ubiquitination and down-stream degradation by the proteasome pathway. The stabilized complex is then able to migrate to the nucleus and promote/inhibit transcriptional activation of p21, p27 and other anti-proliferative effectors (**Figure 3**).

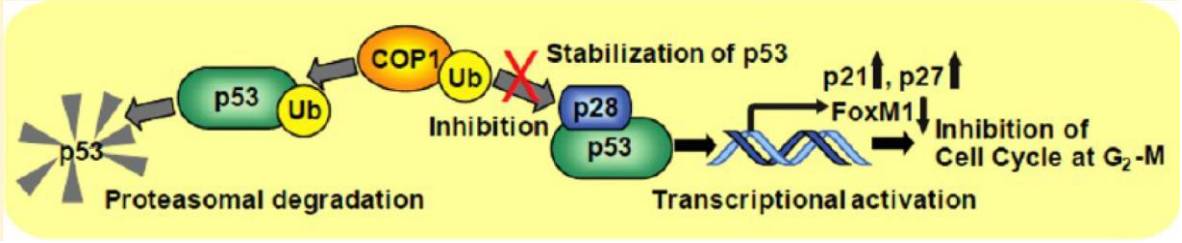

Figure 3 p28 post-translationally interaction with p53 and down-stream effects (extracted from [26]).

Interference with the Eph-Ephrin Pathway

Besides its interaction with p53, azurin likewise targets a cell proliferation pathway mediated by the EphB2 tyrosine kinase [21]. The ephrin-B2 folding topology is a variation on the common Greek key β-barrel fold, which ectodomain is an eight-stranded *β*-barrel arranged in two sheets around a hydrophobic core, and shares considerable topological similarity with the cupredoxin family of copper-binding proteins (including azurin) [27] The root-mean-square deviation of backbone residues between the aligned parts of the pair of structures of azurin (1JZG) and EphrinB2 (1KGY_E) is 3.4 Å with only 5.6% identity and 90 alignment length but with a 10.1 VAST score (out of a 15.7 possible maximum) and a 6.7 DALI Z-score (Z scores measure similarity between the 3D structures, Z < 2.0 are structurally dissimilar) [28].

Surface plasmon resonance (SPR) sensorgrams revealed the relative binding affinity of azurin and various GST-Azurin peptide constructs (all at 100 nM) with EphB2-Fc; azurin > GST–Azu_{88-113} > GST–Azu_{36-128} > ephrinB2-Fc > GST–Azu_{36-89} >>GST. The equilibrium dissociation constants (K_d) of azurin (K_d = 6 nM) and GST–Azu_{88-113} (K_d = 12 nM) had 5- and 2.5-fold higher affinities, respectively, for EphB2-Fc than its native ephrinB2-Fc ligand (K_d = 30 nM). The Azu 88-113 region consists of a G-H loop domain structurally homologous to the G-H loop found in ephrinB2. SPR analysis of binding of EphB2-Fc to ephrinB2-Fc immobilized onto a CM5 sensor chip after pre-incubation with varying

concentrations of azurin and GST–Azu 88-113 indicate a 99% reduction in total protein binding to the surface at stoichiometric and/or excess concentrations of the competitor, while azurin is a slightly more potent inhibitor than GST–Azu 88-113 peptide (±10%) [28]. Azurin has high affinity for EphB2-Fc and it can interfere with ephrinB2-Fc–EphB2-Fc binding by competition with immobilized ligand ephrinB2 binding and receptor occupation.

In vitro, incubation of DU145 prostate cancer cells, with a non-functional EphB2 kinase domain; alone or in the presence of various concentrations of azurin do not show the presence of either phosphorylated tyrosine or EphB2. After being transfection with EphB2 cDNA (~55% transfection efficiency), the addition of increasing amounts of azurin (3.6, 5.4 and 7.1 μM; incubation time not present in the source article) produces an increase in tyrosine phosphorylation, albeit modest. This suggests that azurin binding to the EphB2 receptor allows weak tyrosine phosphorylation in the absence of the natural ligand ephrinB2. Naturally, the electrophoresed immunoprecipitates blotted against anti-P-Tyr of transfected DU145 cells treated with ephrinB2 (0.07, 0.15 and 0.24 μM; incubation time not present in the source article) exuberantly display tyrosine phosphorylation. Most interestingly, an azurin/ephrinB2 (3.6/0.07, 5.4/0.15 and 7.1/0.24 μM) mixture demonstrates a 30-40% lower tyrosine phosphorylation level. Similarly, GST–Azu 88-113 stimulates tyrosine auto-phosphorylation in EphB2 transfected DU145 in the absence of ephrinB2 at concentrations of 0.5 μM or higher. Upon GST–Azu 88-113/ephrinB2 co-treatment (0.25/0.25, 0.5/0.5 and 0.75/0.75 μM), EphB2 kinase domain tyrosine auto-phosphorylation is attenuated in a dose dependent manner (21, 42, and 45%, respectively). These experiments indicate *in vitro* interference of the EphB2–ephrinB2-mediated cell signalling pathway by azurin and Azu 88-113 [28].

Suppression of tumour angiogenesis

Azurin and p28 preferentially enter cancer cells compared with normal cells. In human umbilical vein endothelial cells (HUVEC), p28 penetrates within 30 min and is co-localized with caveolin-1 and vascular endothelial growth factor receptor 2 (VEGFR-2), thus internalization is, at least in part, mediated through caveosome endocytosis [[14], [16], [17], [18], [19], [27]].

However, HUVEC is a non-cancerous but highly prolific endothelial cell line which, upon stimulation with VEGFR-2 and/or basic fibroblast growth factor (bFGF) (both 20 ng/mL) in Matrigel™, forms tubular structures after 24 h of incubation. It also exhibits preferential uptake for azurin and derived peptides compared with human fibroblasts (florescence ~0.5-, 1.5- and 0.75-fold higher, respectively). Furthermore, p28 induces a dose-related inhibition of the number of capillary tube formation stimulated by either vascular endothelial growth factor A (VEGFA) or bFGF alone or in combination (50% inhibition (IC_{50}) at ~12, 100 and 18 μM, respectively). Azurin also inhibits VEGFA and bFGF stimulated tube formation, but far less and only at higher concentrations (IC_{20} of 151, 135 and 145 μM, respectively). Importantly, the inhibition on migration and tube formation do not stem from p28 cytotoxicity effects, since HUVEC exposed to ~250 μM p28 treatments alone do not exhibit cell proliferation inhibition *versus* the controls (using MTT assays) with 24 h exposure [29].

HUVEC incubated in Matrigel™ coated coverslips at 37 ºC for 0.5, 2, 4 and 24 h with VEGFA (20 ng/ml) ± p28 (25 μM) present reposition of actin filaments, focal adhesion kinase (FAK) and paxillin move away from the leading edge of migrating cells and cell periphery to be uniformly

distributed throughout the cell. The majority of platelet endothelial cell adhesion molecule (PECAM-1), also known as CD31, initially located at the cell periphery in HUVEC solely exposed to VEGFA, is re-distributed through the cytosol and returns to the cell periphery after 2-4 h. The addition of p28 alters the intracellular localization of PECAM-1, which remains distributed throughout the cell even 24 h after treatment, towards continued strong cell to cell adhesion phenotype. The induction of intracellular redistribution of structural proteins by p28 in the presence of VEGFA is not accompanied by an overall change in these proteins expression, but present an inhibitory effect in proliferation and angiogenesis through altered distribution of cell-motility and migration associated proteins. Also, p28 produces a non-competitive dose-related decrease (K_i of 7.7 μM) in VEGFR-2 kinase activity (IC_{10} ~ 4.1 μM; and IC_{20} ~ 10.7 μM). As it happens to tube formation, azurin inhibits VEGFR-2 kinase activity but only at higher concentrations (IC_{10} ~ 23.4 μM). pAkt (S473) and pFAK (Y397) are transiently inhibited up to 62% and 55%, respectively, after 30 min exposure to VEGFA (20 ng/mL) and p28 (25 μM), compared to VEGFA alone, however neither the Akt nor the FAK intracellular levels are altered upon exposure to VEGFA with p28 [29].

The above mentioned changes in HUVEC, *in vitro,* were mirrored by a significant reduction in the number of PECAM-1 (CD-31) clusters (N_c; >3 cells) and immune-stained endothelial cells (control: N_c = 5, n = 14.2±2.6 U; p28: N_c = 7, n = 4.3±1.1 U) and reduced bFGF-stimulated capillary growth (white field microscopic analysis) in Matrigel™ implants (0.5 mL Matrigel™, 10 ng VEGFA or 1 μg bFGF; injected subcutaneously in the mid dorsal region) in 5-6 week old athymic mice treated with p28 (16 mg/kg Body Weight (BW) daily for 7 days; 5.5 μM, intraperitoneal injection or 2 mg of p28 in the implant, respectively) [29]. Moreover, p28 (10 or 20 mg/kg BW daily for 15 or 26 days) produced a dose related growth inhibition for UISO-Mel-6 (p53-null; inoculated subcutaneously in the dorsal flank; ~42% and ~31% growth inhibition by volume (V_{p28}/V_{PBS} x100%), respectively) in athymic mice xenografts. Note that BrdU staining suggests that p28 reduced capillary formation ($p < 0.05$), thus indirectly reduce the growth of these p53-null xenograft tumours through reduction in blood supply [29], since p53-null cancer cell such as UISO-Mel-6 are much less sensitive p28 [13].

Modulation of Cell Membrane Properties and invasion

P-cadherin overexpression, in wild-type E-cadherin breast cancer cells (MDA-MB-468 and BT-20), is able to induce increased cell invasion, motility and migration. Additionally, the presence of P-cadherin can provoke the secretion of pro-invasive factors, such as matrix metalloproteases (MMPs), MMP-1 and MMP-2, which leads to P-cadherin ectodomain cleavage and formation of a soluble P-cadherin fragment (sP-cad) responsible for *in vitro* invasion of wild-type E- and P-cadherin expressing cells [30].

In Matrigel™ Invasion Assays, a sub-killing dose of azurin (50 μM; 48 h) impairs invasion of MCF-7/AZ.Pcad and SUM149 (both are invasive cell lines that overexpress P-cadherin) by 66% and 44%, respectively. MCF-7/AZ.Mock cells, which do not overexpress P-cadherin, do not change their non-invasive behaviour after the same azurin treatment and MTT assays performed for the same azurin concentrations and exposure times do not report otherwise decreased cell viability from azurin exposure [31].

Immunofluorescence analysis reveals reduced P-cadherin membrane levels, whereas E-cadherin expression remains unaltered, with normal membrane cell localization. E- and P-cadherin expression levels measured through Western Blot, after azurin treatment (50 and 100 μM; 48 h), reveal that MCF-7/AZ.Mock and MCF/AZ.Pcad decrease in P-cadherin protein levels by 30-50% and SUM19 by 15–30%, while E-cadherin levels are not altered and mRNA levels for CDH1/E-cadherin or CDH3/P-cadherin, observed by quantitative real-time (qRT)-PCR for the same conditions, stay unchanged relative to the controls [31]. According with the decrease in P-cadherin levels at the cellular membrane, a decrease in the sP-cad levels can be observed in the extracellular media (cells grown in a collagen type I matrix) of MCF-7/AZ.Pcad and SUM149 cells 60% and 50%, respectively (azurin 100 μM; 48 h; by WB) with reduction in MMP2 activity by 20 or 40%, and 25 or 60%, respectively (azurin 50 or 100 μM; 48 h by gelatin zymography) [31]. The FAK and Src (proto-oncogene tyrosine-protein kinase) kinase activity is impaired in a P-cadherin overexpression context through an increase in the phospho-FAK and phospho-Src protein levels. Azurin treatment (50 or 100 μM, 48 h) induces a dose-dependent decrease in the phosphorylation levels of both FAK (Y397) (~20% or ~35%, respectively) and Src (Y416) (~30% or ~60%, respectively), with no significant changes in the total proteins levels of these proteins. Unlike in the HUVEC cells, RAC-alpha serine/threonine-protein kinase (Akt), also known as protein kinase B (PKB), phosphorylation (S473) levels do not present any significant change in these P-cadherin overexpressing cell lines [[27], [29]], and any inhibitory effect mediated by azurin does not involve the Akt signalling pathway.

High-throughput molecular profiling in invasive MCF-7/AZ.Pcad cells also support that azurin decreases the expression of genes associated with cell surface receptors and signal transduction, as well as biological adhesion in P-cadherin overexpression cancer cell lines, while apoptosis mediated by p53 protein, endocytosis and vesicle-mediated transport appear to be common targets for eligible cancer cell lines. Gene ontology and enriched pathways (Kegg database) of up- and down-regulated genes in MCF-7/AZ.Mock versus MCF-7/AZ.Pcad cell lines treated with azurin (100 μM, 48 h) and MCF-7/AZ.Pcad, treated relative to untreated cells were analysed with the DAVID software ($p < 0.05$). 415 genes were found to be commonly altered in both cell lines, linked to up regulation of membrane organization, vesicle-mediated transport, endosome transport, lysosome and p53 signalling pathway, and down regulation of genes involved in transcription. Treated relative to untreated MCF-7/AZ.Pcad cells reveal up regulation of vesicle-mediated transport (46 genes), membrane organization (35 genes), induction of apoptosis (34 genes), endocytosis (24 genes), p53 signalling pathway(16 genes) and lysosome (15 genes) genes, and down regulation of cell surface receptor-linked signal transduction (155 genes), biological adhesion (56 genes), response to wounding (48 genes), cell motility (27 genes), cytokine-cytokine receptor interaction (33 genes) and focal adhesions (15 genes) genes [32].

Further studies assessed that azurin decreases adhesion of A549 to Extra cellular matrix (ECM) components and β1 integrin subunit protein expression. A549 is a lung cancer line model for non-small-cell lung carcinoma (NSCLC) with high level expression of wild type epidermal growth factor receptor (EGFR). After treatment with azurin (50 or 100 μM, 48 h), A549 experience a decrease in adhesion to ECM proteins (measured by the crystal-violet assay), such as laminin-332 and collagen

type IV, but especially to collagen type I (20 or 60% decrease in adhesion, respectively) and fibronectin (20 or 50% decrease in adhesion, respectively). For the same single treatment with azurin, under normal plastic conditions, A549 integrin subunit β1 protein expression reduces by 40% and in a matrix formed by collagen type-I condition it reduces by 30% (50 μM azurin) or 70% (100 μM azurin). Inversely, these cells express ~50% higher levels of E-cadherin under the same conditions and ~200% higher levels (3-fold) of E-cadherin in the case of a matrix formed by collagen type-I at 100 μM azurin treatment [33].

In the same study, azurin (100 μM, 48h) is found to impair invasion behaviour in Matrigel^{TM} invasion assays by 30%, with no additional stimuli, and pro-tumorigenic signalling with the phosphorylated levels of non-receptor tyrosine kinases, such as Src and Pi3K/Akt decreasing by ~20, 65 and 60% respectively, without significant total protein levels changing beyond 10% of the control levels, downstream of EGFR. Also azurin treatment (100 μM, 48h) followed by exposure to two concentrations of epidermal growth factor (EGF; 20 and 50 ng/mL, 30 min) show that the levels of phosphorylation in the signalling related residues Y1068 of EGFR fail to increase compared with those of the cells exposed to EGF in the absence of azurin pre-treatment. Hence, azurin leads to a defective response to EGF in A549 cells [33].

Atomic Force Microscopy (AFM) detects increased A549 cell height (~6.5% increase), volume (~23% increase) and area (~8.5% increase), and a decreased membrane stiffness through measurement of the Young's modulus (E; ~30% decrease) induced by azurin treatment (100 μM, 48h), supporting a change from the liquid-ordered to a liquid-disordered membrane state [[19], [31]].

Laurdan fluorescence emission spectra red shift is sensitive to changes in membrane order, by measuring alterations in water molecule penetration within the lipid bilayer and can be quantified by generalized polarization (GP) calculation. MFC-7, HeLa and HT-29 cells treated with azurin WT (100 μM, 30min or 48h) have a decrease in the GP values measured in the plasma membranes, indicating that exposure to azurin causes a decrease in the plasma membrane order. Moreover, the lack thereof, in the same conditions except for treatment with the mutant protein azurin F114A, points that the promotion of decreased membrane order is dependent upon the azurin's hydrophobic patch and/or the C-terminal region of the protein [19].

1.3 Inhibition of Cancer Cell Proliferation and Tumour Growth

1.3.1 Direct cancer cell proliferation inhibition

Besides cell membrane penetration and interference in several independent signalling pathways associated with cancer progression, azurin and its derived peptides have been shown to inhibit proliferation or induce apoptosis in various cancer cell lines. Cancer sensitivity to azurin appears to be closely related with $p53^{+}$ status; however there is a wide range of sensitivity even for p53 WT cancer lines (**Table 1**). *In vivo* experiments in murine models also support the activity of these protein/peptides to produce an effective alternative to conventional chemotherapy treatments (**Table 2**). In addition, recent studies successfully employed azurin to target solid tumours in murine models and two phase 1 clinical trials have been completed (*cf.* subsection 1.4.4).

Table 1 Responses of cancer cell lines to treatment with azurin and derived peptides.

Cancer	Cell Line	p53 Status	Method	Agent (dose; exposure time)	Response (%)	Refs
Breast cancer	MCF-7	WT	Direct cell counting	p28 (50 μM, 72 h)	21±5*	[13]
			MTT	azurin (50 or 100 μM, 72 h)	12±5*, 20±10*	[19]
			MTT	p28 (5, 50, 100 or 200 μM; 24, 48 or 72 h #)	13±5*, 10±3*, 11±1*, 19±5*; 19±4*, 30±3*, 44±5*, 47±5*; 45±4*, 49±3*, 45±2*, 48±2*	[18]
			Cell cycle with PI sub-G0/G1 (apoptosis) phase	p28 (50 μM; 48 or 72 h)	N.E. (-0.8), 21.1*	[18]
			Annexin V and PI staining (early apoptotic, late apoptotic)	azurin (32 μM; 24 h)	34±4' early apoptotic, 21±4' late apoptotic	[24]
			MTT	Azu 88-113 (12.5 μM; 48 h)	47±3''	[28]
	MCF-7/AZ.Mock	WT	Matrigel Invasion Assays	azurin (50 μM; 48 h)	N.E. (-2±25)	[31]
			Mammosphere forming efficiency	azurin (100 μM; 96 h)	22±10*	[32]
			MTT	azurin (50 or 100 μM; 48 h)	8±1*, 19±9**	[31]
	MCF-7/AZ.Pcad	WT	Matrigel Invasion Assays	azurin (50 μM; 48 h)	66±34**	[31]
			Mammosphere forming efficiency	azurin (100 μM; 96 h)	35±5**	[32]
			MTT	azurin (50 or 100 μM; 48 h)	N.E. (1±2), 20±4***	[31]
	MDA-MB-231	Mut	Direct cell counting	p28 (50 μM; 72 h)	20±7*	[13]
			Direct cell counting	p28 (50 or 100 μM; 72 h #)	10±4*, 16±5**	[34]
			Annexin V and PI staining (early apoptotic, late apoptotic)	azurin (32 μM; 24 h)	8±3'' early apoptotic, 10±4'' late apoptotic	[24]
	MDA-MB-157	Null	Annexin V and PI staining (early apoptotic, late apoptotic)	azurin (32 μM; 24 h)	12±3'' early apoptotic, 6±4'' late apoptotic	[24]
	MDD2	Dominant-negative	Direct cell counting	p28 (50 μM; 72 h)	N.E. (-3±7)	[13]
			Cell cycle with PI sub-G1 (apoptosis) phase	p28 (50 μM; 48 or 72 h)	N.E. (0.2; 0.7)	[18]
	SUM-149	Mut	Matrigel Invasion Assays	azurin (50 μM; 24 h)	44±4*	[31]
			Mammosphere forming efficiency	azurin (100 μM; 96 h)	30±2**	[32]

			MTT	azurin (50 or 100 μM; 24 h)	N.E. (-30±12*, -1±12)	[31]
	T-47-D	Mut	MTT	p28 (100 μM; 72 h #)	> 20*	[26]
	ZR-75	WT	Direct cell counting	p28 (50 or 100 μM; 72 h #)	17±5*, 26±4**	[34]
			MTT	p28 (50 or 100 μM; 72 h #)	16±4*, 44±10*	[18]
Cervical cancer	HeLa	WT (low)	MTT	azurin (50 or 100 μM, 72 h)	30±6*, 43±7*	[19]
		Null	Annexin V and PI staining	p28 (0, 0.5, 1 or 2 μM, 24 h)	7±1', 8±1', 9±1'	[37]
Colon Cancer	HCT-116	WT	MTT	p28 (100 μM; 72 h #)	> 20*	[26]
	HT-29	Mut	MTT	azurin (50 or 100 μM, 72 h)	25±2*; 38±1*	[19]
			MTT	p28 (100 μM; 72 h #)	N.E.	[26]
Fibrosarcoma	HT-1080	WT	MTT	p28 (100 μM; 72 h #)	> 20*	[26]
Glioblastoma	LN229	Mut	Direct cell counting	p28 (50 or 100 μM; 72 h #)	13±2**, 12±1***	[34]
			MTT	Azu 88-113 (50 or 100 μM; 48 h)	21±3'', 38±2''	[28]
	U87	WT	Direct cell counting	p28 (50 or 100 μM; 72 h #)	7±2*, 18±3***	[34]
Leiomyosarcoma	HTB-88		MTT	p28 (100 μM; 72 h #)	> 20*	[26]
Lung cancer	A549	WT	Matrigel Invasion Assays	azurin (50 or 100 μM; 48 h)	30±13; 30±7*	[33]
Melanoma	UISO-Mel-2	WT	Direct cell counting	azurin (5, 50, 100 or 200 μM; 72 h #)	3±1''; 13±1''; 24±1'', 55±1''	[14]
			Direct cell counting	p28 (5, 50, 100 or 200 μM; 72 h #)	3±1''; 6±1''; 15±1'', 43±1''	[14]
			Direct cell counting	p18 (5, 50, 100 or 200 μM; 72 h #)	N.E. (0±0''; -1±2''; 1±1'', 2±1'')	[14]
			MTT	azurin (5, 50, 100 or 200 μM; 72 h #)	-1±2''; -5±3''; 15±1'', 13±6''	[14]
			MTT	p28 (5, 50, 100 or 200 μM; 72 h #)	4±2''; -9±2''; 14±3'', 21±4''	[14]
			MTT	p18 (5, 50, 100 or 200 μM; 72 h #)	N.E. (-2±5; -10±5; 4±1, 6±3')	[14]
			MTT	azurin (7.1, 14.3, 28.6 or 57.1 μM; 24 h)	19; 34; 38, 42	[23]
	UISO-Mel-6	Null	MTT	azurin (7.1, 14.3, 28.6 or 57.1 μM; 24 h)	2; 3; 4, 10	[23]
			MTT	p28 (100 μM; 72 h #)	N.E.	[26]
	Mel-23	Mut	Direct cell counting	p28 (100 μM; 72 h)	30±8*	[13]
			Direct cell counting	p28 (50 or 100 μM; 72 h #)	27±7***, 35±3***	[34]
			Direct cell counting	azurin (100 μM; 72 h #)	60±1''	[14]
			Direct cell counting	p28 (100 μM; 72 h #)	50±1''	[14]
			MTT	azurin (100 μM; 72 h #)	45±5''	[14]
			MTT	p28 (100 μM; 72 h #)	22±5''	[14]
			MTT	p18 (100 μM; 72 h #)	N.E. (-3±10'')	[14]

	Mel-29	WT	Direct cell counting	p28 (100 μM; 72 h)	24±4*	[13]
			Direct cell counting	p28 (50 or 100 μM; 72 h #)	17±4***, 22±3***	[34]
			Direct cell counting	azurin (100 μM; 72 h #)	40±4''	[14]
			Direct cell counting	p28 (100 μM; 72 h #)	34±2''	[14]
			MTT	azurin (100 μM; 72 h #)	47±4''	[14]
			MTT	p28 (100 μM; 72 h #)	27±8''	[14]
			MTT	p18 (100 μM; 72 h #)	16±3''	[14]
Neuroblastoma	IMR-32	WT	Direct cell counting	p28 (50 or 100 μM; 72 h #)	25±1***, 33±2***	[34]
	SK-N-BE2	Mut	Direct cell counting	p28 (50 or 100 μM; 72 h #)	24±7***, 35±3***	[34]
Oral squamous carcinoma	YD-9	WT	MTT	azurin (14.3 μM; 24, 48 or 72 h)	25±3*; 45±3*; 50±5*	[35]
Osteosarcoma	MG-63	Null	MTT	azurin (14.3, 28.6 or 57.1 μM; 48 h)	8±2'', 10±3'', 10±3'', 12±2''	[25]
			MTT	azurin (14.3 μM; 24, 48 or 72 h)	N.E.	[35]
	TE-85	Mut	MTT	p28 (100 μM; 72 h #)	N.E.	[26]
	U2OS	WT	MTT	azurin (14.3, 28.6 or 57.1 μM; 48 h)	48±4*; 58±3; 60±3', 62±2'	[25]
			Annexin V and PI staining (apoptotic)	azurin (14.3 μM; 48 h)	36±3''	[25]
Ovarian cancer	ES-2	Mut	MTT	p28 (100 μM; 72 h #)	N.E.	[26]
Pancreatic cancer	MIA-Paca2	Mut	MTT	p28 (100 μM; 72 h #)	N.E.	[26]
Prostate cancer	LNCaP	WT	Direct cell counting	p28 (50 or 100 μM; 72 h #)	7±2*, 18±2***	[34]
	DU-145	Mut	Direct cell counting	p28 (50 or 100 μM; 72 h #)	12±1*, 22±2***	[34]
			MTT	azurin (0.01, 0.1 or 1 μM; 48 h)	N.E.	[28][28]
			MTT	Azu 88-113 (0.01, 0.1 or 1 μM; 48 h)	N.E.	[28]
Rhabdomyosarcoma	RD	Mut	MTT	p28 (100 μM; 72 h #)	N.E.	[26]

Positive values correspond to inhibition, while negative values correspond to increased growth compared with the controls. p53 status: WT, wild-type; Mut, mutated.
', Standard Deviation (SD), '', Standard Error of the Mean (SEM), *, $p < 0.05$, **, $p < 0.01$, ***, $p < 0.001$, N.E. - no/negative effect. # active compound was replenished daily.

Table 2 Responses of cancer cell lines to treatment with azurin and derived peptides in murine models.

Cancer	Cell Line	p53 Status	Model	Method	Agent (dose; exposure time)	Response (%)	Refs.
Breast cancer	MCF-7	WT	5- to 6-week-old male and female athymic mice	s.c. injection in the right flank %tumour weight/PBS control	p28 (10 or 20 mg/kg i.p. 3 /week for 30 days)	60±10*, 53±1*	[13]
	MDA-MB-231	Mut	5- to 6-week-old male and female athymic mice	s.c. injection in the right flank %tumour weight/PBS control	p28 (10 or 20 mg/kg i.p. 3 /week for 30 days)	N.E., 56±18*	[13]
			5- to 6-week-old female athymic mice	s.c. injection in the right flank %tumour weight/PBS control	azurin (10 mg/kg i.p. daily for 30 days)	70±18*	[34]
Dalton's lymphoma	DL	WT	male Swiss mice	i.p. injection %cell survival/PBS control	azurin (50, 100 or 200 µg/kg 3 /week for 10 days)	30±1***, 64±4*** 89±1***	[36]
Melanoma	UISO-Mel-2	WT	male nude mice	s.c. injection in the right flank %tumour volume/PBS control	azurin (25 mg/kg i.p. daily for 22 days)	60±23'	[23]
			5- to 6-week-old male athymic mice	s.c. injection in the right flank %tumour volume/PBS control	azurin (4 mg/kg i.p. daily for 16 days)	37±7*	[34]
	UISO-Mel-6	Null	5- to 6-week-old male and female athymic mice	s.c. injection in the right flank %tumour weight/PBS control	p28 (10 mg/kg i.p. 3 /week for 30 days)	N.E.	[13]
	Mel-23	Mut	5- to 6-week-old male and female athymic mice	s.c. injection in the right flank %tumour weight/PBS control	p28 (10 or 20 mg/kg i.p. 3 /week for 30 days)	61±17*, 52±16*	[13]
			5- to 6-week-old male athymic mice	s.c. injection in the right flank %tumour volume/PBS control	azurin (5 or 10 mg/kg i.p. daily for 30 days)	33±28*, 58±24*	[34]
	Mel-29	WT	5- to 6-week-old male and female athymic mice	s.c. injection in the right flank %tumour weight/PBS control	p28 (10 or 20 mg/kg i.p. 3 /week for 30 days)	43±25*, 50±16*	[13]

Positive values correspond to inhibition, while negative values correspond to increased growth compared with the controls. p53 status: WT, wild-type; Mut, mutated.
', Standard Deviation (SD), '', Standard Error of the Mean (SEM), *, $p < 0.05$, **, $p < 0.01$, ***, $p < 0.001$, N.E. - no/negative effect.

1.4 Azurin and derived peptides: Research and Clinical trials state of the art

Azurin and derived peptides preferentially enter human cancer cells, inducing cell cycle arrest or apoptosis through interference with several relevant independent signalling pathways, or inhibit angiogenesis in tumours. Based on these anti-proliferative activities, several therapeutic strategies have been designed.

1.4.1 Therapeutic Drugs

Ghasemi-Dehkordi *et al.* (2019) constructed a DNA recombinant vector plasmid (pBudCE4.1-azurin-MAM-A) to express azurin and Mammaglobin-A in order to induce immune responses against breast cancer tumours in BALB/c mice. In the study, the DMBA and MNU chemical compounds were used for induction of breast cancer. Treatment with the DNA construct pBudCE4.1-azurin-MAM-A both reduces the rate of breast tumour incidence (3/12 treated versus 10/11 control) as well as the mean mammary tumour weight (345±3 mg treated versus 723±7 mg control), in mice that exhibit tumour formation. In addition, immune induction responses against breast cancer tumours were observed with the doubling of cytokines relative expression (IFN-γ, IL-4, IL-12 and IL-17). The ultimate goal, in future studies, is the application of this recombinant vector as a DNA vaccine to treat and prevent breast cancer in humans [38]. On the other hand, Shahbazi *et al.* (2018) complexed the HPV16 E7 protein with p28 (20:1 nanoparticles, 1 μg E7 protein), and demonstrated that the construct efficiently produces and immunological response that targets cervical cancer cells in 5–7 week old C57BL/6 female mice, upon three inoculations with a 2-week intervals. Two weeks after the third vaccination, the mice were s.c. injected with 1×10^5 TC-1 tumour cells (cell line prepared from primary murine lung epithelial cells co-transformation with HPV16 E6 & E7 and Ras oncogenes) in the right flank, and all displayed complete regression and remained tumor-free >60 days following it [39].

Besides possible DNA vaccines other approaches are also promising. Bacterial therapy may allow intratumoral production of cytotoxic drugs thus reducing toxicity to normal cells while concentrating the cytotoxic compounds in the cancer tissue microenvironment [21]. Zhang *et al.* (2012) demonstrated the combined therapeutic effects of the azurin and bacterial anticancer activity through the administration of *Escherichia coli* Nissle 1917 (EcN) that expressed and secreted azurin. EcN Nissle 1917 has tumour-targeting ability, hence preferentially accumulated within the necrotic areas of the tumours with 10^9 CFU/g within, versus less than 100 CFU/g in intact tissues, 3 days after i.v. administration of the bacterium in a safe dose (2×10^7 CFU). Inoculated female BALB/c and C57BL/6 mice, 6 to 8 weeks, old bearing B16 melanoma or 4T1 breast tumour models presented marked delay in tumour progression and prolonged survival by about 50% (IC_{50} at approximately 25 and 55 days *vs.* 15 and 45 days to the controls). Furthermore, the number of pulmonary metastatic nodes for 4T1 breast tumours is reduced by 41±31% ($p < 0.05$) after 30 days of treatment, compared with either PBS or EcN not expressing azurin control groups [40]. Mehta *et al.* (2017) designed a *S. typhimurium* strain VNP 20009 (ATCC 202165) carrier that simultaneously expresses azurin and p53 under the control of a hypoxic promoter. In this experiment, 80,000 human U87 MG GBM cells (ATCC

HTB-14) were injected in adult male athymic RNU rats, 2.0 mm lateral and 2.0 mm anterior to bregma to a depth of 2.0 mm in the left cortex. Two responses were observed in the treated rat group, 19.4% (responders) presented a survival extending beyond 100 days (until they were euthanized), and the rest (non-responders) died within the same time frame as the controls (IC_{50} 30 days, last non-responder died at day 40) [41].

1.4.2 Anticancer Drug Sensitizers

Another avenue for therapy explores azurin and associated peptides to enhance sensitivity in combined application with anti-proliferative chemotherapeutic agents. Bernardes and colleagues found that azurin enhances the sensitivity of A549 lung cancer cells to gefitinib and erlotinib [33], of MCF-7 and HeLa cells to paclitaxel and of HT-29 to paclitaxel and doxorubicin [19]. Gefitinib (1 μM) co-treatment with Azurin (100 μM) resulted in a ~10% viability decrease compared with the sum of the isolated responses at 72 h of treatment (15±10% and 32±10%, respectively), without statistical synergy. However and more interestingly, treatment with Azurin/Gefitinib (100/0.01 μM) decreased cell viability 3-fold over the treatment with Gefitinib (1 μM) alone. The co-response with erlotinib (1 μM), presented a ~8% A549 viability decrease in the same conditions (32±16% and 22±2%, respectively), with ~9% statistical synergy [33]. Synergistic sensitivity of MCF-7 breast cancer cells to Azurin/Paclitaxel occurs for 50/0.1 μM/nM, with a ~13% viability decrease compared against the sum of the isolated responses at 72 h of treatment (12±6% and 8±2%, respectively), corresponding to ~14% synergetic effect. In HeLa cervical cancer cells, Azurin/Paclitaxel 100/0.1 μM/nM and 100/0.5 μM/nM treatments present the same viability decrease within the error margins. Although there is not proper statistical synergy (less than 3% and within error margins), again, for the same response there is a 5-fold paclitaxel dose reduction. In HT-29 colon cancer cells, Azurin/Paclitaxel synergy occurs at all combinations of 50, 100/0.1, 1 μM/nM, with ~9% decreased viability corresponding the synergetic effect between drugs and ~75% decreased viability for 100/0.1, 1 μM/nM. Regarding the effects of the Azurin/Doxorubicin combined treatments, there is ~16% decrease in viability corresponding the synergetic effect between drugs for 50/10 μM/nM, also there is synergy at all combinations of 50, 100/10, 50 μM/nM but to a lesser extent [19]. It is relevant to state that azurin and its peptides by themselves have very low toxicity while in the medium to non-cancerous cells even at very high concentrations (e.g. HUVEC exposed to ~250 μM p28 treatments do not lose viability [29]) since their uptake is reduced. Gefitinib, erlotinib, paclitaxel and doxorubicin are quite nefarious drugs for any normal mitotic cell type, thus even if the viability decrease is not synergistic this approach can be useful for reducing the doses of the current chemotherapy protocols. For example, while the combined effect of azurin (100 μM) and gefitinib (0.01 μM) in A549 cells is not synergistic, it is nevertheless ~3-fold that of the gefitinib (1 μM), thus for the addition of a very well tolerated drug it is possible to reduce the gefitinib dose more than 100-fold [33].

Furthermore, azurin enhances sensitivity of YD-9 oral squamous carcinoma cells and MG-63 cells to 5-fluorouracil (5-FU) and etoposide. Oral squamous carcinoma cells are resistant to these drugs, so finding a way to enhance the sensitivity of these cells to anticancer drugs is important in order to avoid surgical therapy (the primary treatment for oral cancer), which can cause facial

distortion. YD-9 presents ~90% or ~80% viability loss 24 h upon combined treatment with 14.3/10 μM azurin/5-fluorouracil or 14.3/3.4 μM azurin/etoposide, against ~10% corresponding loss in viability for 5-FU or etoposide treatment alone. Similar results are obtained while using MG-63 (p53-null) cancer cells. Given that azurin alone does not have a cytotoxic effect on p53-null MG-63 cells, this indicates that azurin can enhance the sensitivity of MG-63 cells to 5-FU and etoposide in a p53-independent manner [35].

Yamada *et al.* (2016) found that combined application with p28 improves the activity of DNA damage drugs (doxorubicin, dacarbazine, temozolamide) and antimitotic drugs (paclitaxel and docetaxel) in a variety of cancer cells (prostate cancer, LNCaP, DU145, PC-3; neuroblastoma, IMR-32, SK-N-BE2; breast cancer, ZR-75, MDA-MB-231; glioblastoma, U87, LN229; melanoma, Mel-29, Mel-23) [34].

1.4.3 Cancer-Targeted Drug Carriers

Other therapeutic applications can be found from the preferential targeting/entry of azurin and derived peptides into cancer cells. The preferential entry of azurin and derived peptides into cancer cells enables them to function as cancer-targeted drug carriers.

The use of chimeric proteins containing p28 for selective entrance into cancer cells has been used to enhance the cytotoxic activity of other peptides. For instance, NRC is an antimicrobial peptide with cytotoxic activity towards even drug-resistant breast cancer cell lines but it also presents high cytotoxicity towards normal cells. The chimeric p28-NRC (8 μM, 48h) construct has been shown to increase sensitivity of MCF-7 and MDA-MB-231 up to a 90% loss of viability compared to the 40% lost for HUVEC through MTT assays. Additionally, ~40% of MCF-7 cells treated with IC_{50} (1.88 μM) of chimeric protein for 4 h were found to be in early apoptosis and another 40% in late apoptosis through annexin V and PI cytometric staining analysis [42].

Furthermore, the ability of azurin to bind to ephrin receptors has been used to engineer peptide-nicotinamide conjugates in order to increase radiotherapy sensitivity in tumours. Micewicz *et al.* (2011) prepared a small peptide library comprised of azurin fragments between amino acids 88–128 and screened their binding affinity to the Eph receptors EphA2, EphB2, and EphB4 using SPR. Moreover, modifications such as introduction of charged residues and increased hydrophobicity were developed to further improve binding affinity. Then, the best element from the library was optimized to additionally enhance solubility and stability at physiological conditions and was conjugated to nicotinamide. The finalized construct, AzV36-Nic, and its linear form, AzV36-NicL, displayed the best binding affinities, in the nanomolar range [43]. Afterwards, two in vivo models, an artificial metastasis model and solid tumour engraftment model, were used to assess the sensitizing activity of these derived peptides. In both models, the peptides achieved a ~13-fold increase in radiotherapy efficacy in treatment versus the controls [43].

Paydarnia *et al.* (2019) designed a granzyme B-azurin fusion protein that also induces significant apoptosis induction in MDA-MB-231, MCF7 and SK-BR-3 cells (IC_{50} of 136, 19 and 92 μM, WST-1 assay, 72 h; and 79, 65.6 and 39.8% increase in DNA fragmentation, [^{3}H]-thymidine release,

16 h; respectively), while presenting insignificant cytotoxicity towards MCF-10A normal breast cells (70+% cell viability at 500 μM) [44].

1.4.4 Human phase-1 clinical trials

Following the safety profile of azurin and derived peptides two phase I clinical trials with p28 have been proposed and recently completed, with findings confirming anticancer activity and safety of the peptide in human cancer patients.

The first one (NSC745104), selected fifteen stage IV cancer patients with histologically or radiologically proven metastatic refractory solid tumours resistant to conventional therapeutics of diverse histogenesis (seven melanoma, four colon, two sarcoma, one pancreatic, and one prostate), verified as p53-positive tumours (primary or metastatic) and with a possible life expectancy of no more than 6 months. Also, a minimum of 4 weeks elapsed since completion of any prior form therapy; adequate baseline organ function; adequate cardiac and pulmonary function were required. Upon acceptance the patients were sequentially enrolled to receive p28 administered as an i.v. infusion over 15–30 min three times per week for four weeks followed by a 2-week rest period, each starting at one of five progressively higher dosage (*i.e.*, 0.83 mg/kg, 1.66 mg/kg, 2.5 mg/kg, 3.33 mg/kg or 4.16 mg/kg). After p28 treatment, none of these patients showed any significant toxicity effects for any dose, seven demonstrated stable disease for 7–61 weeks, three showed partial response for 44–125 weeks, and one showed complete response for 139 weeks. At the time of publishing these findings three patients were still alive at 158, 140, and 110 weeks post therapy completion [45].

The other clinical trial (NSC745104) was performed with eighteen eligible children aged 3–21 years with histologically confirmed progressive, recurrent, or refractory high-grade glioma, medulloblastoma, primitive neuroectodermal tumours, atypical teratoid rhabdoid tumour (AT/RT), diffuse intrinsic pontine glioma (DIPG), or choroid plexus carcinoma (all are central nervous system tumours) for whom no curative therapy exists. p28 was i.v. administered three times per week for four consecutive weeks in a six-week cycle at 4.16 mg/kg/dose (the adult recommended phase II dose). Although, p28 was deemed safe and well tolerated, no complete or partial responses were observed [46].

2 Motivation

The mechanisms of action of azurin are diffuse, involve increased uptake into cancer cells and metabolic modulation in multiple pathways, and for the most part are somewhat understood. But the relation between metabolic modulation, reduced proliferation and detection of apoptotic indicators (*e.g.* Bax/Bcl2), and actual cell death is very lacking. In cancer cells, the plasma membrane microdomains (e.g. Lipid rafts) act as platforms to many proteins with aberrant constitutive signalling, such as integrins and receptor tyrosine kinases. Azurin may dislodge/reorganize the membrane receptors there located, hampering the signalling through which they promote cancer progression. This research work aims to contribute to the elucidation of the anticancer effect of azurin regarding the induction of cell death and membrane disruption in a lipid raft-dependent process. It proposes to carry out the following studies:

a) Analysis of the effect of azurin on the inhibition of cell proliferation in different types of human cancer cell lines of different tissue origin.

b) Analysis of the effect of azurin on the induction and extent of cell death in different types of human cancer cell lines of different tissue origin, and characterization of the cell death process.

c) Analysis of the putative involvement of membrane microdomains in the cell killing action of azurin in cancer cells.

The current developments sound promising in better understanding the multi-faceted role of azurin in cancer therapies. Moreover, studies with other amphipathic molecules like edelfosine and the previously described antiparasitic activity in azurin might relate to the anti-cancer properties of these molecules and can further be studied.

3 Materials and Methods

3.1 Bacteria growth, over-expression, extraction and purification of WT azurin or mutated F114A protein

The continuous production of azurin was performed as described in Bernardes *et al.* (2013) [31].

3.1.1 Bacteria and Growth Media

Succinctly, a previously cloned *Escherichia coli* SURE strain with the plasmid pWH844, containing the *azu* gene or the one containing the F114A mutation, from *Pseudomonas aeruginosa* PAO 1, which is responsible for the synthesis of azurin, placed downstream of its T7 promoter was inoculated in a 250 mL Erlenmeyer flask containing 100 mL of Luria Broth medium (LB medium) and 100 µL ampicillin at an 150 µg/mL concentration. The SURE strain is proteases expression deficient, thus it is suitable for protein overexpression. This pre-inoculum was incubated overnight with agitation, at 250 rpm and 37 ºC and cultured, in the next morning, at an initial optical density of 0.1 at 640 nm (OD640), in 3 L Erlenmeyer flasks containing 1 L Super Broth medium (SB medium; 20 g/L of yeast extract, 32 g/L of triptone and 5 g/L of NaCl) supplemented with 150 µg/mL ampicillin with the same growing conditions. Upon reaching stable exponential growth, at an OD640 of 0.6-0.8, IsoPropyl-21β-D-ThioGalactopyranoside (IPTG, inductor of azurin's promoter; Sigma Life Science) was added to the culture at a final concentration of 0.2 mM for Azurin WT and 0.5 mM for Azurin F114A, and the culture was left growing for an additional 4-5 h while maintaining the same conditions. After this time, cells were harvested by centrifugation (8000 rpm, 10 minutes, 4 ºC; Beckman J2-MC Centrifuge); the resulting pellet was re-suspended in 15 mL of Start buffer (10 mM imidazole, 0.2 mM sodium phosphate, 0.5 M NaCl, pH 7.4). Cells were stored at -80 ºC for further use.

3.1.2 Protein Purification

The cells were disrupted (mechanical lysis of cell walls and membranes) by sonication (Branson Sonifier Sound Enclosure250) and the purification steps were performed by histidine affinity chromatography, using HisTrap^{TM} HP columns (GE Healthcare), since the *azu* gene was cloned into a plasmid with a 6 histidine tail tag nucleotide sequence. Briefly, the disrupted cells were twice centrifuged (17600x g, 5 and 60 minutes, respectively, 4 ºC; B. Braun Sigma-Aldrich 2K15), the pellets, consistent of cellular debris, were discarded after each cycle and the supernatant recovered. Then, the clarified extract was loaded into a 5 mL HisTrap HP column equilibrated with START buffer. Protein elution was achieved with a continuous imidazole gradient (from 20 to 500 mM) in the same buffer. After purification, the protein was immediately desalted and buffer exchanged to phosphate buffered saline (PBS; 137 mM of NaCl, 2.7 mM of KCl, 4.3 mM of $Na_2HPO_4.2H_2O$ and 1.47 mM KH_2PO_4, pH 7.4), in a HiPrep 26/10 Desalting column (GE Healthcare) in an ÄKTA purifier system (ÄKTA Start, Cytiva, USA), following the manufacturer's instructions. The collected protein was

concentrated by centrifugation (5000 rpm, 4 ºC; Eppendorf Centrifuge 5804R) with Amicon Ultra Centrifugal Devices (Milipore), with a 10 kDa molecular mass cut-off. The final volume of purified protein was centrifuged in a 100 kDa cut-off filter, to remove eventual contaminants. Protein concentration was assessed spectrophotometrically at 280 nm with the azurin specific peak at 292 nm. The purity of protein was analysed by sodium dodecyl-polyacrylamide gel electrophoresis (SDS-PAGE). Test spot assays were performed overnight at 37 °C (two spots with 10µL of azurin in a LB agarplate) to verify microbiological sterilization. Azurin was stored at 4 ºC until further use.

3.2 Cell cultures

Three human cancer cell lines and one normal baby hamster cell line was used in this work: HeLa (ATCC CCL-2, human cervix adenocarcinoma), AGS (ATCC CRL-1739, human gastric adenocarcinoma), U2OS (ATCC HTB-96, human osteosarcoma) and BHK-21 (ATCC CCL-10, hamster kidney fibroblast). All cell lines were maintained at 37 ºC in 5% CO_2. HeLa, U2OS, BHK-21 were grown in DMEM (GIBCO™, Paisley, UK) and AGS's was grown in (1:1) DMEM/F12 (GIBCO™) culture medium, supplemented with 10% (v/v) heat-inactivated fetal bovine serum (FBS) (GIBCO™), 2 mM L-glutamine (GIBCO™), 100 U/mL penicillin and 100 µg/mL streptomycin (PenStrep, GIBCO™) at 37 °C in humidified 95% air and 5% CO_2 (Binder CO_2 incubator C150). Cells were passage by chemical detaching with Trypsin 0.05% upon reaching ~80% confluence both for maintenance and for experiment initialization. 12.5 µg/mL ciprofloxacin (Sigma-Aldrich) was added into the above mentioned culture media to avoid Mycoplasma contamination.

3.3 Cytotoxicity assays

3.3.1 MTT cell viability assay

MTT [3-(4,5 dimethylthiazol-2-yl-2,5 tetrazolium bromide)] assays were used to determine the proliferation rate of HeLa, AGS, U2OS cell lines after treatment with azurin WT and F114A. The assays were performed in 96-well plates (Corning Inc., NY, USA) (at least 3 replicates x3) with densities of 1.5×10^3 HeLa cells/well, 1×10^3 AGS cells/well, 1×10^3 U2OS cells/well in 100 µL culture medium. The cells were left to adhere and grow overnight at 37 °C in a humidified 95% air and 5% CO_2 incubator. In the next day, azurin treatments with set doses (from 25 to 200 µM according to the specific experiment) were added from a stock concentrated solution (~650 µM azurin in PBS); PBS and medium only controls were also set to ensure that the increased total volume and respective dilution of culture medium did not affect proliferation. The plates were placed in the incubator for 72 h at 37 °C. After, 10 µL of MTT reagent (5 mg/mL) was added to each well and incubated for an additional 4 h at 37 °C. Thereafter, the reaction was stopped by carefully removing the medium and addition of 100 µL of spectrometric grade pure DMSO (Dimethyl sulfoxide; Sigma-Aldrich, St. Louis, MO, USA). MTT formazan formed was spectrophotometrically read at 595 nm in a microplate reader (iMark™ microplate reader, Bio-Rad, Hercules, CA, USA).

3.3.2 PI Incorporation and Cell cycle analysis

Propidium iodode (PI) incorporation assays by flow cytometry were used to determine cell membrane permeability and for quantitative determination of apoptosis through analysis of DNA fragmentation in HeLa, AGS, U2OS and BHK-21 cell lines. The cells were seeded in 24-well plates (Corning Inc.) with densities of 2.5×10^4 HeLa cells/well, 1.5×10^4 AGS cells/well, 1.5×10^4 U2OS cells/well and 1.5×10^4 BHK-21 cells/well in 1 mL. The cells were left to adhere and grow overnight at 37 °C in a humidified 95% air and 5% CO_2 incubator. In the next day, medium was changed and cells were treated with azurin WT or F114A at 100 µM from stock concentrated solutions (~650 µM azurin in PBS) added to the specific cell culture medium in order to achieve 500 µL of total volume. The plates were placed in the incubator for 72 h at 37 °C. After the incubation time the cells were centrifuged (Eppendorf 5804 R) (1200 rpm, 5 min). Half were then suspended in 400 µL of PBS in ice and immediately stained with 5 µg/mL PI (Sigma-Aldrich) and analysed by flow cytometry (Cytomics FC 500 Flow Cytometer, Beckman Coulter Inc., Brea, CA, EUA) for PI incorporation and the other half were fixed overnight in 700 µL of 70% ethanol at 4 °C. In the following day, cells were washed and centrifuged (Megafuge 2.0R, Controltecnica Instrumentacion Cientifica S.L., Spain) two times with PBS (1mL), incubated at least for 30 min with 1 mg/mL RNase A and 12.5 µg/ml PI at room temperature as previously described in Gajate *et al.* (2000) [47], and then analysed for cell cycle with a Cytomics FC 500 (Brea, CA) flow cytometer. Quantitation of apoptotic cells was calculated as the percentage of cells in the sub-G1 region (hypodiploidy) in cell cycle analysis. All raw data was analysed using the Cyflogic version 1.2.1 software and compiled in a spreadsheet at Microsoft Office Excel 2010.

4 Results

4.1 Azurin inhibits proliferation in HeLa, AGS and U2OS cells

Cell viability through MTT assays decreased in a dose dependent manner, with cell arrest up to 80% for HeLa (human cervix adenocarcinoma) at 200 µM, 95% for AGS (human gastric adenocarcinoma) at 200 µM and 57±15% for U2OS (human osteosarcoma) at 100 µM, 72 h after treatment with azurin (**Figure 4**). Due to experimental limitations and azurin availability all further assays were performed at 100 µM, for which 42±22% and 62±17% proliferation inhibition was observed for HeLa and AGS, respectively. Values are presented as mean ± SD.

Inhibition of proliferation is slightly higher for "p53 positive", with emphasis at 100 µM, although there was no statistical significance ($p > 0.05$) between "p53 Null" status (HeLa) and "p53 positive" status (AGS and U2OS). All tested cell lines present a positive dose response with a decrease in viability. This suggests that the azurin´s cytotoxic/cytostatic must go beyond the activation of the p53 mediated cell arrest pathway, thus supporting the hypothesis that azurin presents a multi-targeted low specificity interaction with different metabolic pathways leading to cell viability loss.

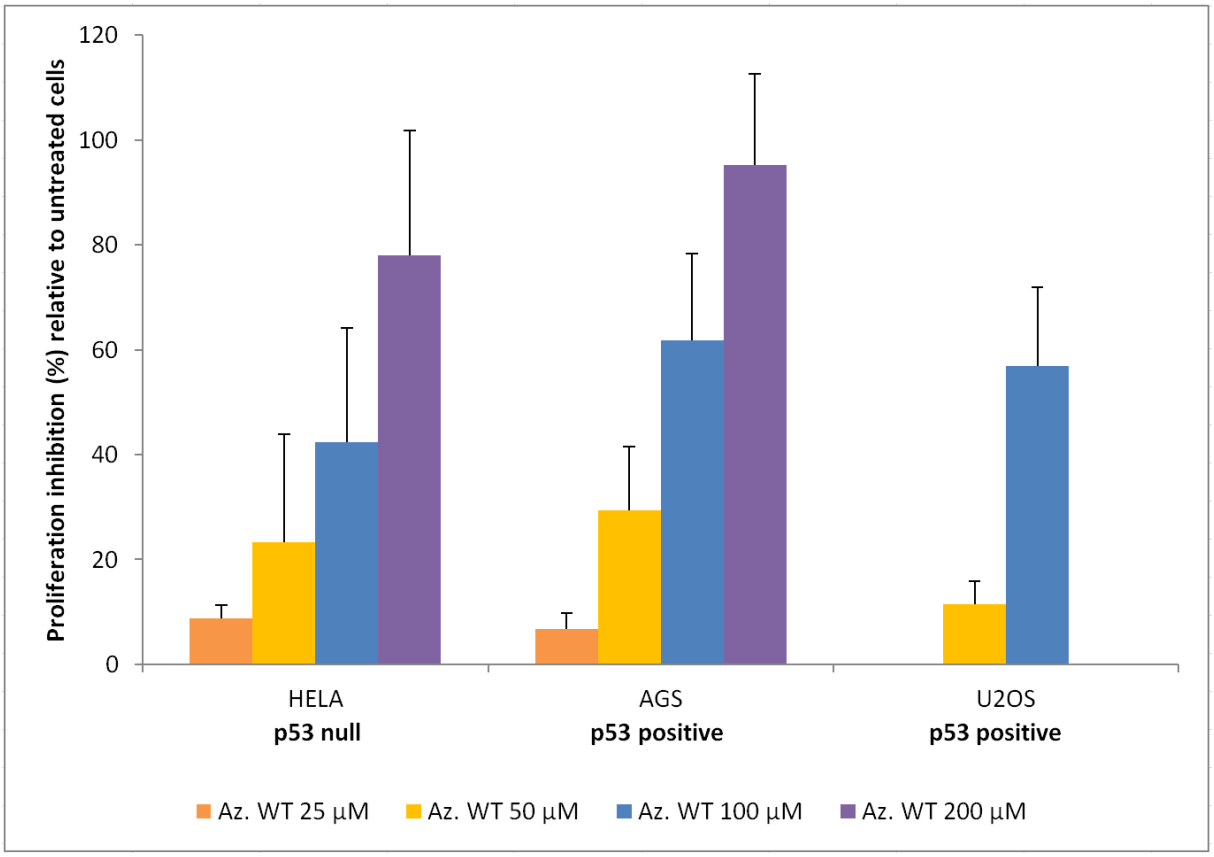

Figure 4 Azurin inhibits proliferation in HeLa, AGS and U2OS cells. Azurin (25, 50, 100 or 200 µM) decreases cell proliferation in a dose dependent manner. 1.5×10^3 HeLa cells per well, 1×10^3 AGS cells per well and 1×10^3 U2OS cells per well were plated in 96-well plates and left to adhere overnight. In the next day, cells were treated with 25, 50, 100 or 200 µM of azurin, 100 µL of total volume. After 72 h, cell proliferation was determined by MTT assay. Results are expressed as the percentage of formazan crystals spectral absorbance at 595 nm of azurin treated cells relative to the control (untreated cells). Values are presented as mean ± SD. All bars have statistical significance related to untreated cells ($p < 0.05$).

4.2 Azurin promotes membrane destabilization with pore formation in cancer cell lines

To evaluate the interaction and cell membrane disruption in azurin-treated cells, PI incorporation was measured by Flow cytometry in freshly harvested cells. In order to maintain homeostasis the membrane needs to be selectively permeable with only small non-charged molecules being able to freely diffuse through it without meditated uptake. PI is a red-fluorescent that is not permeant to live cells or cells with an intact cell surface, in homeostatic conditions. It can be used to detect dead cells (PI binds to DNA). Thus, the uptake of PI indicates that the cell surface is partially disrupted or has become permeant. Therefore, PI incorporation is a direct measure of membrane integrity and cell viability. Only cells with loss of metabolic function or with abnormal pore/ micro-pore formation are positively detected to incorporate PI by Flow cytometry (FL3 wavelength).

HeLa, AGS, U2OS and BHK (non-cancer hamster kidney line) cells presented 30.1±9.1%, 37.4±3.2%, 21.5±5.6% and 10.9±0.9% PI permeable populations, respectively, upon treatment with 100 μM azurin WT at 72 h (**Figure 5**). Statistical significance ($p < 0.05$) in respect to the controls was achieved for AGS, U2OS and BHK, and $p = 0,066$ for HeLa. Base control incorporation was ~12%, 17%, 9% and 1%, respectively.

Moreover, in order to understand the role of the azurin hydrophobic patch in the formation of micro pores, the same cell lines were treated with the point mutant F114A (100 μM, 72 h). HeLa, AGS, U2OS and BHK cells presented 16.4±6.4%, 45.9±5.0%, 19.9±10.6% and 10.3%* PI permeable populations, respectively. These results are in line with the observations made regarding hypoploid populations in the cell cycle. The azurin mutant produces an increase in the permeabilization relative to the controls. However, there is no consistency of effect between azurin F114A and WT, across all cell lines.

These results point that azurin contributes to the destabilization of the cell membrane (at least for HeLa and AGS) with the formation of pores upon long exposure (72 h) to azurin beyond what could be expected from the proportion of cell death. Also, BHK-21 cells are less susceptible than the cancer cell lines with statistical significance for HeLa and AGS ($p < 0.01$). Note that previous studies with MCF-7/IUSO-Mel-2 shown that short term (10 min) exposure to azurin does not lead to membrane pore formation even at very high concentrations (250 μM azurin, LDH assay) [14]. Therefore, there must be an intrinsic mechanism through which azurin promotes cellular membrane instability either through direct interaction and adsorption with the membrane or through modulation of cellular pathways related with membrane integrity. The later hypothesis is supported by some previous publications [[14], [33]].

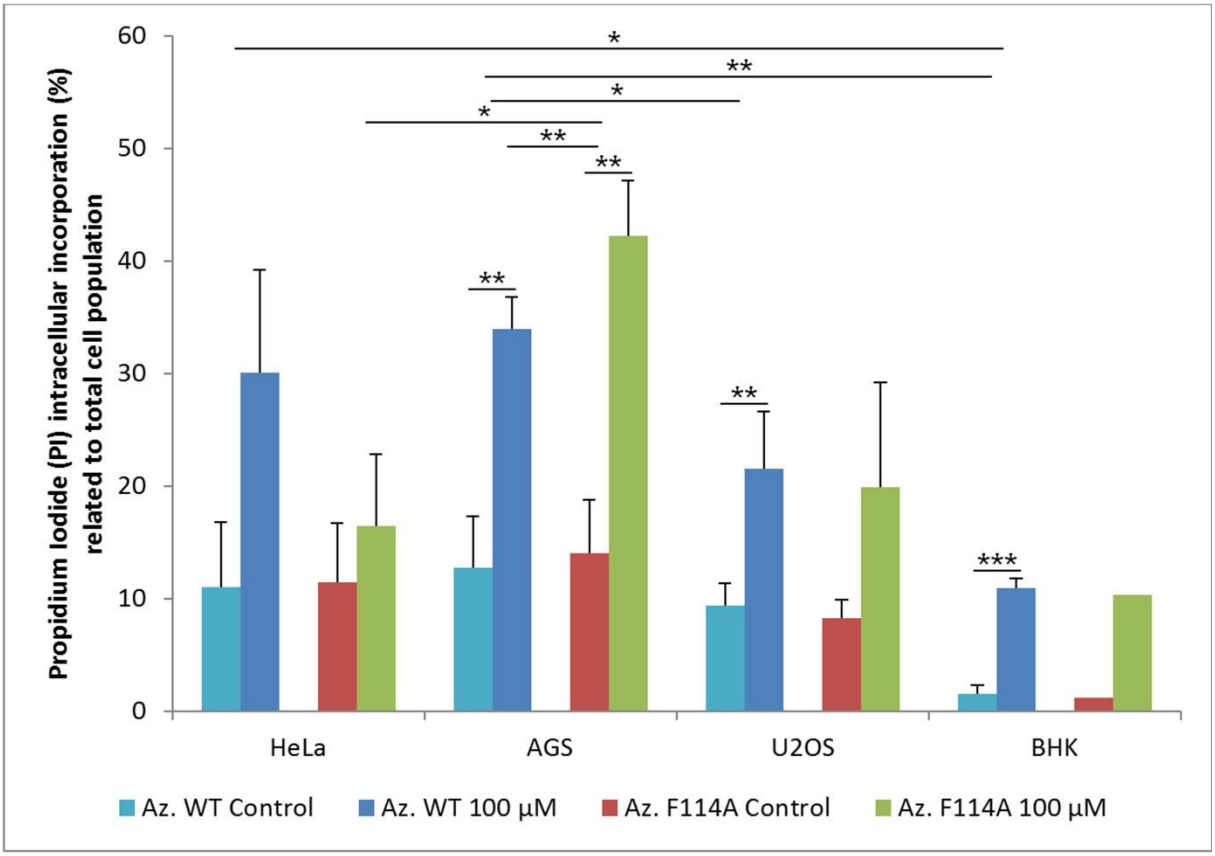

Figure 5 Effect of azurin WT and F114A in Propidium Iodide (PI) intracellular incorporation. Azurin WT and F114A at 100 µM differentially increased PI incorporation levels in HeLa, AGS, and U2OS versus BHK cells. 2.5×10^4 HeLa cells per well, 1.5×10^4 AGS cells per well, 1.5×10^4 U2OS cells per well and 1.5×10^4 BHK-21 cells per well were plated in 24-well plates with 1 mL medium and left to adhere overnight. In the next day, cells were treated with either azurin WT 100 µM or azurin F114A 100 µM, 500 µL of total volume. After 72 h of incubation time at 37 °C, the cells were centrifuged (1200 rpm, 5 min), suspended in 400 µL of PBS in ice and immediately stained with 5 µg/mL PI and analysed by PI-FL3 flow cytometry. Results are presented as the percentage of PI positive relative to the total cell population for the given cell line. The dark blue bars represent cells treated with azurin WT, the green bars represent cells treated with azurin F114A and the light blue and red bars represent their respective controls (untreated cells). Values are presented as mean ± SD. The asterisks over each bar represent statistical significance related to untreated cells; the asterisks over a line connecting 2 bars represent statistical significance between those 2 conditions (*$p < 0.05$; **$p < 0.01$; ***$p < 0.001$). BHK treated with azurin F114A had no replicas, thus data were statistically invalid.

4.3 Azurin increases the hypoploid population levels in cancer cells

Although several studies have been undertaken that demonstrate azurin's preferential anti-proliferation efficacy towards cancer cells with studies performed in vitro and in vivo using animal models with minimal toxicity to non-cancer cells [[17], [18]], there is a lack of understanding in the amount of death (presumably through apoptosis) that azurin is capable to produce both *in vitro* and *in vivo*.

In order to evaluate the cell death induced by azurin, flow cytometry assays with PI in treated cells fixed in ethanol were produced and the results are shown in **Figure 6** and **Figure 7**. HeLa, AGS, U2OS and BHK cells present 6.2±4.6%, 14.9±4.6%, 6.8±3.9% and 4.6±0.8% hypoploid populations, respectively, (corresponding to dead cells with fragmented DNA) upon treatment with 100 µM at 72 h

of azurin WT. Statistical significance ($p < 0.05$) in respect to the controls was achieved for AGS, U2OS and BHK.

Also, previously Bernardes *et al.* (2018) proved a reduction in azurin penetration for short incubation times up to 2 h in cancer cells, when the protein´s hydrophobic patch was disturbed due to the point mutation F114A [19]. Thus to assess if said penetration reduction propagated into cell cycle abnormalities or increased cell death, the same procedure as stated in the previous paragraph was performed but while using azurin F114A instead. HeLa, AGS, U2OS and BHK cells present 6.9±3.2%, 20.6±9.4%, 2.7±0.7% and 4.9%* hypoploid populations, respectively upon treatment with 100 µM at 72 h of Azurin F114A (**Figure 6**). Therefore, for long exposure times and for high dosage the cytotoxic effect of azurin F114A is statistically the same as the effect produced with azurin WT ($p > 0.1$ for all cell lines).

These results point to a previously not known moderate cytotoxic effect of azurin in the AGS cell line that might further be explored in gastric cancer therapeutics research.

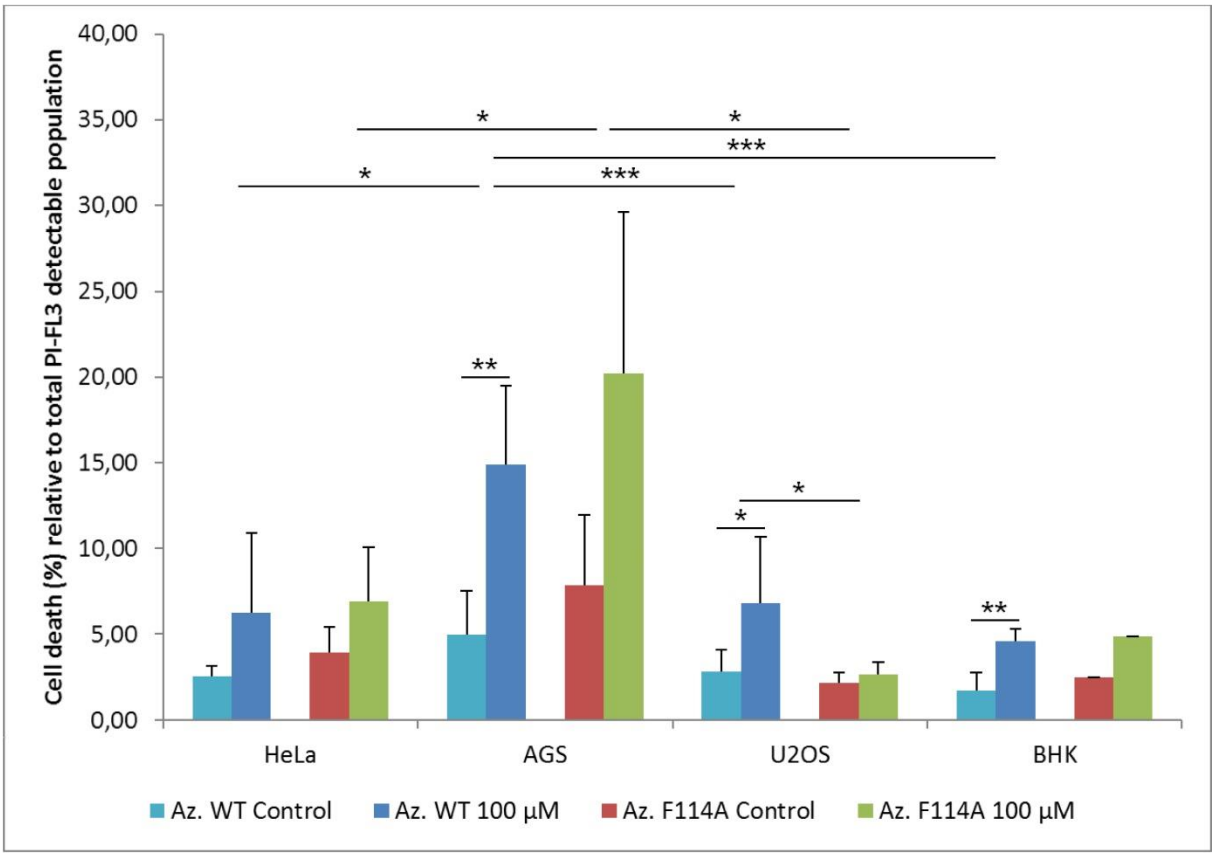

Figure 6 Effect of azurin WT and F114A in the cell death. Azurin WT at 100 µM increases the hypoploid population levels (apoptotic or late-necrotic cells) in cancer cell lines (HeLa, AGS, and U2OS) more than in the non-cancer cell line (BHK), with emphasis in the Cav-1^{-}/p53^{+} AGS primary gastric cancer line. Azurin F114A at 100 µM increases the hypoploid population levels in all cell lines similarly to azurin WT ($p > 0.1$). 2.5×10^4 HeLa cells per well, 1.5×10^4 AGS cells per well, 1.5×10^4 U2OS cells per well and 1.5×10^4 BHK-21 cells per well were plated in 24-well plates with 1 mL medium and left to adhere overnight. In the next day, cells were treated with either azurin WT 100 µM or azurin F114A 100 µM, 500 µL of total volume. After 72 h, the cells were harvested and fixed in ethanol 70% at 4 ºC. Results are presented as the percentage of the hypoploid population (sub-G0/G1) in relation to the total population by PI-FL3 flow cytometry. The dark blue bars represent cells treated with azurin WT, the green bars represent cells treated with azurin F114A and the light blue and red bars represent their respective controls (untreated cells). Values are presented as mean ± SD. The asterisks over each bar represent statistical significance related to untreated cells; the asterisks over a line connecting 2 bars represent statistical significance between those 2 conditions (*$p < 0.05$; **$p < 0.01$; ***$p < 0.001$). BHK treated with azurin F114A had no replicas, thus data were statistically invalid.

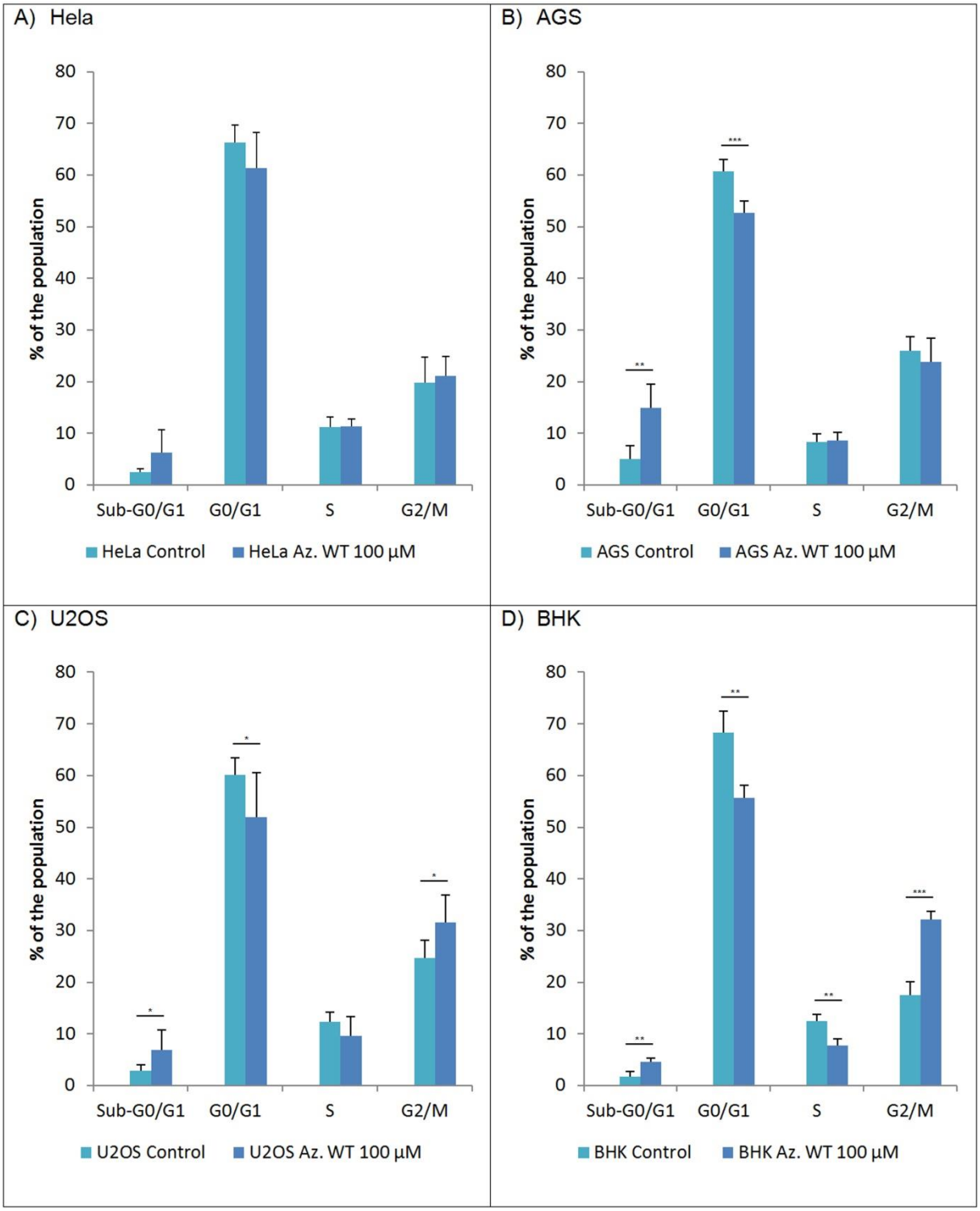

Figure 7 Effect of azurin in the cell cycle. Azurin at 100 µM increases the hypoploid population levels (apoptotic or late-necrotic cells), in detriment of the main stage population (G0/G1), in (A) HeLa; (B) AGS; and (C) U2OS; versus (D) BHK cells. 2.5×10^4 HeLa cells per well, 1.5×10^4 AGS cells per well, 1.5×10^4 U2OS cells per well and 1.5×10^4 BHK-21 cells per well were plated in 24-well plates with 1 mL medium and left to adhere overnight. In the next day, cells were treated with azurin 100 µM, 500 µL of total volume. After 72 h, the cells were harvested and fixed in ethanol 70% at 4 ºC. Results are presented as the percentage of the total population encompassed in each cell cycle phase (sub-G0/G1, G0/G1, S and G2/M) by PI-FL3 flow cytometry. The dark bars represent cells treated with azurin and light bars represent the controls (untreated cells). Values are presented as mean ± SD. The asterisks over each bar represent statistical significance related to untreated cells; the asterisks over a line connecting 2 bars represent statistical significance between those 2 conditions (*$p < 0.05$; **$p < 0.01$; ***$p < 0.001$).

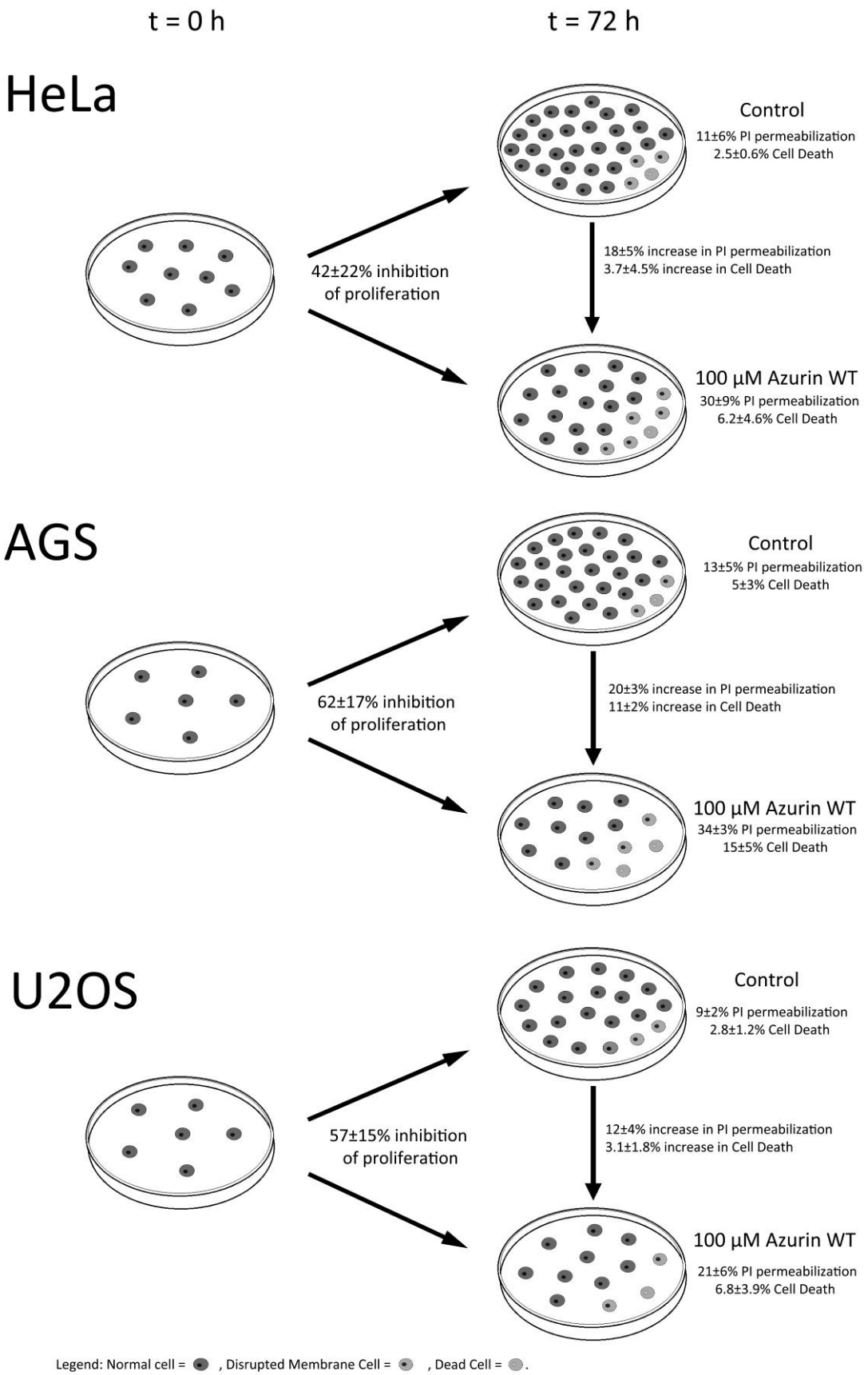

Figure 8 Pictorial representation of the combined cytostatic and cytotoxic effects of 100 µM azurin at 100 µM in HeLa, AGS, and U2OS. The number of cells are roughly to scale comparing between each experimental condition, however only the seeding numbers (t = -24 h) were ensured (*cf.* section 3.3).

5 Discussion

Azurin is a small protein from P. aeruginosa shown to directly target cancer cells, with extensive metabolic alterations in multiple pathways.

Cupredoxins such as rusticyanin, plastocyanin, azurin/azurin-like have been studied extensively for their electron transfer properties [[48], [49]]. More recently they emerged as a natural (*i.e.* not synthetically constructed) proteins with anti-cancer properties. The copper-containing redox protein azurin is a small 14 kDa protein naturally occurring in *P. aeruginosa* that can enter preferentially enter human cancer cells and induce either apoptosis or inhibition of cell cycle progression [[23], [24]]. The mechanisms of action of this protein are diffuse, involve increased uptake into cancer cells and metabolic modulation in multiple pathways, and for the most part are somewhat understood (*cf.* section 1.2.3). But the relation between metabolic modulation, reduced proliferation and detection of apoptotic indicators (*e.g.* Bax/Bcl2), and actual cell death is very lacking. Thus raising the question: Do the previously observed metabolic modulation, inhibition of proliferation and the increased detection of apoptotic indicators relate to actual percentage of cell death in the population? And if so, how much cell death is present upon treatment with azurin?

Cell death measurements using PI-Flow cytometry or equivalent have been previously assessed in breast cancer using azurin (in MCF-7, MDA-MB-231 and MDA-MB-157) [24] and p28 (in MCF-7 and MDD2) [18], osteosarcoma (U2OS; azurin) [25] and cervix cancer (HeLa; p28) [37]. In general the experiments were performed to evaluate the apoptosis of $p53^{+}$ *versus* $p53^{-}$/$p53^{mut}$ cancer cell lines. In the conditions that were set by the respective research groups $p53^{+}$ cancer lines were the most sensitive with 20-60% while $p53^{mut}$/ $p53^{-}$ at most showed 10% cell death and more often than not there was no death at all (for details *cf.* **Table 1**, section 1.3). In regards to the extent of cell death, the present results contradict previous published data and raise some doubts on the real ability of azurin to promote apoptosis efficiently. Even taking into consideration the use of much higher azurin concentrations and longer treatment durations than in previous research, there was less cell death than expected for $p53^{+}$ cancer cells (AGS and U2OS) and more cell death than expected for the $p53^{-}$ cells (HeLa) (**Figure 6**). Note that HeLa was the only cancer line that did not achieve statistical significance ($p < 0.05$) relative to the controls (untreated cells). For unknown reasons, in this work, the observed cell death in U2OS induced by azurin was far inferior (~7% *vs.* ~35% with 100 µM, 72 h *vs.* 14.3 µM, 48 h, respectively) than the one observed in the findings produced by Yang *et al.* (2005) [25]. Possible explanations for this disparity might be specific experimental setups and laboratory intrinsic variabilities. The experiments in this work were carried out in the presence of ciprofloxacin, a Mycoplasma inhibitor in order to avoid contamination, which could affect cell sensitivity to azurin in both ways (some cells might become very sensitive to certain drugs, while others become resistant).

Consistency of azurin in inhibition of proliferation vs inductor of apoptosis

According to Hanahan and Weinberg [50], cancer cells exhibit six important physiology changes: (1) self-sufficiency in signals of growth, (2) insensitivity to signals inhibiting growth, (3) resistance to apoptosis, (4) unlimited proliferative potential, (5) sustained angiogenesis and (6) metastasis. Regardless of the p53 status, all cancer lines demonstrated a significant dose dependent inhibition in proliferation measured through MTT assays (**Figure 4**). Therefore, it appears that the

cytostatic effect of azurin is mostly independent of p53 status, but the cytotoxic effects leading to cell loss of function (cell death) are dependent. Thus, it is reasonable to consider that most other metabolic pathways deemed to be involved in the anti-cancer activity of azurin are more related with inhibition of proliferation without apoptosis (or any other cell death mechanism) than with direct cytotoxic action of the protein.

Prior findings support this notion that the properties of azurin involved in anti-cancer progression rely in mechanisms beside direct induction of cell death and reversion of resistance to apoptosis (3), such as interference with the Eph-Ephrin pathway (4) [28], tumour angiogenesis suppression (5) [29] and modulation of cell membrane and adhesion/invasion properties (2 and 6) [[30], [31], [32]]. Neither of which are directly related with total loss of cellular function, but rather cell arrest due to modulation of gene transcription, endogenous and exogenous inhibition of proliferation and morphological disturbances impairing metastatic phenotypes both at the membrane and cytoskeletal levels.

In this work, the azurin treatment achieved very low induction of cell death in cancer cell lines (**Figure 6**), in itself insufficient to be consider as an effective standalone drug to be used in cancer therapies in the future. However, the combined modest cell death induction with the much more accentuated anti-proliferative effect (**Figure 8**) might prove to be effective in slowing, or even arresting (in especially azurin sensitive tumours), the progression of the disease.

Loss of membrane integrity in cancer cell lines

Previously, Bernardes *et al.* (2016 and 2018) demonstrated that azurin modulates membrane properties of lung cancer cells with altered morphological features, namely a reduced Young's modulus (E) and an increase in cell area, height and volume, analysed by Atomic Force Microscopy (AFM) imaging and Nano-indentation measurements [33] and increased membrane fluidity in colon (HT-29), cervix (HeLa) and breast (MCF-7) cancer lines, due to the azurin's interaction with the lipid raft components ganglioside GM-1 and caveolin-1 [19]. Regardless of how altered were the membrane properties, direct measurements of integrity remained undetermined.

The results hereby presented demonstrate the loss of membrane integrity with substantial increase in population permeability to propidium iodide (PI) for all cancer cell lines (**Figure 5**), whereas the non-cancer cell line (BHK), employed as a control, presented a smaller PI permeable population. Furthermore, this pore/micro-pore formation seems to be the result of intracellular metabolic modulation rather than direct destabilization of the membrane due to membrane adsorption. If adsorption, owing to the high concentration treatment, were the main contributor to membrane destabilization and pore formation then all cell lines (cancer and non-cancer) would have been similarly affected. Interestingly, the azurin F114A mutant, previously shown to have lower fluorescence resonance energy transfer (FRET) efficiency to the Caveolin Scaffolding Domain (17% *vs.* 35% for the WT) and not decrease membrane order [19], produced similar membrane permeabilization to PI in the population as the WT (**Figure 5**). This further suggests intracellular metabolic modulation as a mechanism of membrane destabilization that is, at least partially, independent of direct interaction with lipid raft components and depletion of Caveolin. Note that although the uptake rate of azurin F114A mutant in cancer cells is lower than it is for the WT counterpart, for long treatment durations the total

uptake imbalance becomes much less accentuated [19], and thus, with longer exposures, the intracellular effects of the mutant should became similar to the WT ones.

Comparison of cancer versus non-cancer cell lines

In the current work, azurin shows preferential effect towards the promotion of cytoplasmic membrane disruption (**Figure 5**) and cell death (**Figure 6**) in cancer cell lines (HeLa, AGS and U2OS) compared with the non-cancer cell line, BHK. This goes in accordance with the findings by Yamada *et al*. (2005 and 2009) where the researchers found a strong preference in internalization of azurin and p28 (p28 is the azurin's protein transduction domain (PTD)) in diverse cancer lines in detriment of their non-cancerous counterparts [[14], [17]]. Additionally, there is evidence that azurin has the ability to induce apoptosis once inside normal cells. Upon microinjection with the protein (7 μM, 0.5 s injection time and 100 hPa pressure) normal fibroblast and MCF-10F cells (non-cancer cell line) present significant nuclear condensation and fragmentation after 5 h [17]. Therefore, it is reasonable to assume that the increase in the intracellular concentration of azurin due to increased permeability in cancer cells is responsible for the differential increase in cell death and membrane disruption observed between the cancer and non-cancer cell lines. However, experiments in non-cancer cell lines with intracellular levels of azurin comparable with those found inside cancer lines upon azurin exposure have never been made (*i.e.* are not in the literature). Microinjection or transfection assays might be used to clarify the assumption that **at the same level** once inside, azurin has the same metabolic effects and cytotoxicity regardless cell cancer status given that the metabolic pathways affected by the protein are present in all lines, but both methods have problems in applicability when trying to investigate for a large cell count population.

Note that, the previous notion that caveolae-mediated endocytosis in Lipid rafts is central to the internalization of azurin [[14], [19]] might be incomplete at least for very long treatment durations. The AGS Cell line does not express Caveolin-1 (Cav-1$^-$) (beyond what is measurable through Western Blot and RT-PCR) or any Caveolin subunit [51], but it is the most sensitive line from the ones tested and the intracellular content Western Blot of treated AGS clearly shows that azurin is present intracellularly (result not shown, due to unforeseen circumstances stemming from the COVID-19 Pandemic). It is relevant to point that the aforementioned researchers tested for 1 h maximum exposures and at <20 μM concentrations and not 100 μM at 72 h, as is the case in the current work.

Azurin is a natural protein with anti-cancer cytotoxic activity with comparable effect to most alternative natural occurring, non-target specific synthetized molecules.

In general, anti-cancer drugs with high affinity to a specific target can either induce death (or indirect toxicity) in normal cells or chemo resistance in the highly metabolic/genetically instable cancer cells [52]. Thus, in the past decades, new approaches have been thought in order to attempt to surpass these hurdlers. Many, as is the case of azurin, revolve around the use of natural occurring molecules, proteins and peptides of bacterial origin, with cytotoxic properties, such as antibiotics (*e.g.* Actinomycin D from *Actinomyces antibioticus*; and Doxorubicin from *Streptomyces peucetius* var. *caesius*), toxins (*e.g.* Botulinum neurotoxin type A from *C. botulinum*; Diphtheria toxin from *C. diphtheriae*; and Exotoxin A from *P. aeruginosa*), enzymes (*e.g.* Arginine deiminase from *Mycoplasma hominis* and *M. arginine*; and L-asparaginase from *Escherichia coli* and *Erwinia* sp.), and

proteins/peptides involved in metabolism (*e.g.* Entap from *Enterococcus* sp.; and Pep27anal2 from *S. pneumoniae*) [53]. The current sub-section is dedicated to the comparison of the previously stated cytotoxic and cytostatic static effects of azurin relative to other notable bacterial products and even products of mammalian secretion with emphasis on proteins/peptides.

As previously stated, azurin has a diffuse mode of action leading to its cytotoxic and cytostatic properties in cancer cells. This promiscuity for its target receptors, as well as the preferential intake observed in cancer cells with apparently minor side effects, points to possible novel approaches to cancer therapies with reduced risk of resistance to therapy.

The results show that azurin has little toxicity towards the non-cancer cell line (**Figure 6**), while having a higher statistically significant toxicity towards the $p53^{+}$ lines, especially in AGS. In addition, all cancer cell lines display extensive proliferative inhibition, with natural tendency for increased inhibition in the lines where toxicity is higher. Therefore, it is arguable (given the unfortunate organizational inability to procure enough azurin to perform MTT assays for the non-cancer cell line) that azurin even at high doses[16] (100 μM) does not present major proliferative disruption in normal cells, while producing at least its anti-proliferative effects in its targets. This allows for avenues where azurin could be used in very high doses, assuming an otherwise compliance with safety, in order to inhibit tumour proliferation *in vivo*. Thus, potentially avoiding the common side effects present in the current clinically used cytostatic drugs, such as Doxorubicin (DOX), which also inhibits normal cell proliferation leading, for example, to alopecia or damage to most naturally proliferative epithelia [52].

The most highly effective and widely used in medicine antitumor active antibiotics, besides DOX: Actinomycin D (dactinomycin), Bleomycin (BLM) and Mitomycin C; have the same problems regarding side effects as DOX. Bernardes *et al* (2018) [19] demonstrated synergistic anti-proliferative effect between azurin and DOX in HT-29 colon cancer cells. For the same durations and concentrations used in this present work it was possible to archive the same loss of viability with a fifth of the concentration of DOX. Thus, azurin might be used to reduce traditional chemotherapeutic doses while providing the same anti-tumour benefits, with the added reduction of the former's side effects.

Toxins, such as exotoxin A or the diphtheria toxin (DT), have been shown to possess anticancer activity in both experimental models and humans [53]. These toxins work having similar mechanisms of action. Both arrest cell protein synthesis, thus leading to cell death [[54], [55]]. They are always used in clinical practice, as an anti-cancer therapy in conjunction with other substances given their adverse side effects [56].

Some enzymes have also been found to possess anticancer activity. The anti-tumour action of bacterial arginine deiminize (ADI) and L-asparaginase (ASNase) is due to their ability to deplete their respective amino acid and thus reduce its blood concentration, causing a selective inhibition of growth of sensitive auxotrophic malignant cells. However, especially in the case of ADI, these enzymes are strongly antigenic in their native form; with a very short 5 h half-life. Though, PEGylated ADI (ADI-PEG20) can decrease antigenicity and increase serum half-life [53].

[16] The maximum dose in clinical trials using the derived peptide p28 has been ~1.4 μM per kg bodyweight [45].

Additionally, the analogues of Pep27, a secreted peptide that initiates the cell death program in *S. pneumoniae* through signal transduction, have been found to possess very interesting similarities to azurin or the derivate peptide p28 according to author of the present work, especially Pep27anal2. While the anticancer cytotoxic activity of Pep27anal2 is reported to be caspase and cytochrome *c* independent, this 3.3 kDa peptide adopts a stable α-helical conformation in solutions and presents increased hydrophobicity, which appears to play an important role in its membrane permeabilization as a cell-penetrating peptide (CPP) [57], just as azurin and p28 have been reported to be [[14], [16], [17]]. Most Pep27 analogues inhibit proliferation of leukaemia (AML-2, HL-60, Jurkat), gastric cancer (SNU-601) and breast cancer (MCF-7) cell lines, assessed through MTT assays. The researchers showed that Jurkat cells exposed to 62.5 μM of Pep27anal2 for 4 h (concentrations comparable with the ones used in current work) had significant induction of apoptosis and late necrosis with dual staining for annexin V-FITC (FL1-H) and PI (FL2-H) by FACS assay [57]. Lee *et al.* (2005) propose that "Pep27anal2 is a potential candidate for anticancer therapeutic agents" [57]. Unfortunately, no research could be found regarding the effects Pep27 and its analogues have in normal cells, *in vitro*, and their safety, *in vivo* models.

Other examples of protein-based anti-tumour therapies exist in the literature based instead on human proteins or peptides, also acting as CPP exerting pro-apoptotic effects in cancer cells. Lactoferrin (Lf) and its derived peptide lactoferricin B (Lfcin) are mammalian nutraceutical protein/peptide with iron-binding ability, with demonstrated activity against a broad spectrum tumour types, including HeLa and AGS [58]. Although, several studies suggest that exogenous treatment with Lf and its derivate peptides can efficiently inhibit the growth of tumours and reduce susceptibility to cancer, cytotoxicity is reported to occur in distinct ways under different conditions, namely by cell membrane disruption, apoptosis induction, cell cycle arrest, and cell immunoreaction [59]. In this respect, lactoferrin and azurin, both appear to present their effects in a diffuse and promiscuous manner (*cf.* section 1.2.3). Relevantly for comparison with the results obtain in this work, lactoferricin B25 (LFcinB25), a 25 amino acid cationic peptide fragment, has been demonstrated to exhibit anticancer capability against AGS cells at 64 μM for 24 h with up to 46% apoptosis by ethanol fixed PI-FL2 flow cytometry. According to Western blot findings LFcinB25 induced caspase-dependent apoptosis of AGS cells via both intrinsic and extrinsic pathways [60]. Another peptide derived from bovine lactoferricin with six amino acids, bLFcin6, demonstrated cargo deliver ability, such as siRNAs, to the interior of cancer cells through a lipid raft-dependent micropinocytosis [61]. This ability to deliver cargo to the interior of cancer cells appears to be quite common in CPP and as CPP in their own right both p28 and azurin have been demonstrated to also be able to deliver cargo to the interior of cancer cells [[17], [42], [43], [44]].

Azurin as a targeting tumour targeting molecule

As stated immediately above, azurin as a CPP has been demonstrated be able to deliver cargo to the interior of cancer cells. Previously, the cancer cells penetration ability of azurin/p28 containing complexes has been closely associated with the notion of the amphipathic characteristics associated with the protein and the presence of the hydrophobic patch surrounding the copper biding active centre [[10], [11]] and its interaction with caveolin-1 in lipid rafts [[14], [19]]. As stated before in this

discussion, caveolae-mediated endocytosis in Lipid rafts might provide an incomplete picture in the internalization of azurin in cancer cells given the results obtained for the AGS cell line (**Figure 5** and **Figure 6**). These observations combined open prospects to use azurin or p28 as cancer targeting molecules even for cancer devoid of caveolin-1 expression.

Azurin mode of action and its relevance in cancer therapy

Azurin by itself seems to have cytostatic and some cytotoxic properties, although the direct cytotoxic effects are somewhat lacking, at least in accordance to the results hereby presented (**Figure 4** and **Figure 6**). Azurin appears to have a diffuse mode of action and given the degree of cytostatic/cytotoxic effects it seems more reasonable to be used as a co-adjuvant with other anti-cancer drugs, such as DOX or Paclitaxel (PTX) than stand alone as observed by Bernardes *et al.* (2016 and 2018) whom proposed the use of azurin in cancer therapeutics as a mean of dose reduction in widely used chemotherapeutic drugs in hopes of mitigating the severe side effects of said drugs [[19], [33]]. Also the low toxicity observed towards non-cancer cells allows azurin for use in therapeutic settings if economically viability and regulatory approval is achievable. In other words, evidence points that azurin might have tangible benefits in tumour progression *in vitro* and *in vivo* models (*cf.* sections 1.3 and 4.3) and the clinical trials preformed to the moment using the derived peptide p28 [[45], [46]], for all intents and purposes indicate safety in the use of the protein/peptide, thus there is good reason to contemplate their use as co-adjuvant or as a biotechnological platform in other to deliver chemotherapeutic constructs selectively to tumours.

6 Conclusions

Azurin is a small protein from P. aeruginosa shown to directly target cancer cells, with extensive metabolic alterations in multiple pathways. Previously azurin has been deemed a cytostatic drug and this work corroborates said finding in all studied cell lines. Although the metabolic differential effects of azurin in cancer cells are somewhat understood its relation with total cell death are not. This study elucidates the extent of cell death promoted by azurin in three cancer cell lines (HeLa, AGS and U2OS). The results obtained in this work support previous research results about the metabolic actions that azurin elicits in cancer cells, however some findings contradict them, such as the amount of death in U2OS. These discrepancies may be related to specific experimental setups and laboratory intrinsic variabilities (e.g. specific azurin treatment regiment, azurin stability after transport from Lisbon to Madrid), which could have significantly affected the outcome of the experiments. The adding of ciprofloxacin to the culture media ensured the avoidance of Mycoplasma contamination in the current work. Membrane integrity was evaluated and it was confirmed that azurin disrupts cell membranes and furthermore disrupts differentially cancer lines membranes. By itself the protein seems to have very relevant cytostatic properties mediated through several metabolic pathways and some cytotoxic properties, although the direct cytotoxic effects are somewhat lacking, at least in accordance to the results obtained in the current work. However, a previously not known moderate cytotoxic effect of azurin was observed in the AGS cell line, which might be further explored in gastric cancer therapeutics research. Azurin appears to have a diffuse mode of action and given the degree of cytostatic/cytotoxic effects that were observed, it seems more reasonable to use this protein as a co-adjuvant with other anti-cancer drugs than stand alone. As a cell-penetrating protein, azurin can also be used as a tumour targeting molecule and since in this exploratory work it has shown to produce the most cytotoxic effect in a Cav-1- cell line, it is likely that the targeting mechanism is effective beyond the previous found association with caveolin-1 mediated vesicular endocytosis in lipid rafts. Future avenues of research in biotechnology pose azurin as an engineering enabler suitable for development for targeted pharmaceuticals such as transfection of tumour tropic Mesenchymal Stem Cells, bioengineering of truncation products and bioactive nanoparticles.

References

[1] World Health Organization, “Cancer,” Updated 12 December 2018. Retrieved April 2020.

[2] Burden of Disease Collaborative Network. Global Burden of Disease Study 2017 (GBD 2017) Results. Seattle, United States: Institute for Health Metrics and Evaluation (IHME), 2018.

[3] Ferlay J, Colombet M, Soerjomataram I, Mathers C, Parkin DM, Pineros M, Znaor A, Bray F, “Global and Regional Estimates of the Incidence and Mortality for 38 Cancers: GLOBOCAN 2018,” Lyon: International Agency for Research on Cancer/World Health Organization, 2018.

[4] Bray F, Ferlay J, Soerjomataram I, Siegel RL, Torre LA, Jemal A, (2018), “Global cancer statistics 2018: GLOBOCAN estimates of incidence and mortality worldwide for 36 cancers in 185 countries,” *CA: A Cancer Journal for Clinicians*, pp. 68: 394-424, 2018.

[5] Global Burden of Disease Study 2015 Risk Factors Collaborators, “Global, regional, and national comparative risk assessment of 79 behavioural, environmental and occupational, and metabolic risks or clusters of risks, 1990–2015: a systematic analysis for the Global Burden of Disease Study 2015,” Lancet, pp. 388:1659–1724, 2016.

[6] Crosta P, “Cancer: Facts, Causes, Symptoms and Research,” Medical News Today, Updated 24 Nov 2015.

[7] Zheng HC, “The molecular mechanisms of chemoresistance in cancers,” *Oncotarget*, pp. 8:59950–59964, 2017.

[8] Hojjat-Farsangi M, “Small-molecule inhibitors of the receptor tyrosine kinases: promising tools for targeted cancer therapies,” *International Journal of Molecular Sciences*, pp. 15:13768–13801, 2014.

[9] Vonderheide RH, K. L. Nathanson KL, “Immunotherapy at large: the road to personalized cancer vaccines,” *Nature Medicine*, vol. 19, no. 9, pp. 1098–1100, 2013.

[10] Fialho AM, Salunkhe P, Manna S, Mahali S, Chakrabarty AM, “Glioblastoma multiforme: novel therapeutic approaches.,” *ISRN Neurology*, pp. 2012:642345, 2012.

[11] C. Jeuken LJ, Ubbink M, Bitter JH, van Vliet P, Meyer-Klaucke W, W. Canters G, “The structural role of the copper-coordinating and surface-exposed histidine residue in the blue copper protein azurin,” *Journal of Molecular Biology*, pp. 299:737–755, 2000.

[12] Santini S, Bizzarri AR, Cannistraro S, “Modelling the interaction between the p53 DNA-binding domain and the p28 peptide fragment of Azurin,” *J Mol Recognit*, pp. 24:1043–1055, 2011.

[13] Yamada T, Christov K, Shilkaitis A, Bratescu L, Green A, Santini S, Bizzarri AR, Cannistraro S, Gupta TK, Beattie CW, ”p28, a first in class peptide inhibitor of cop1 binding to p53,” *Br J Cancer*, pp. 108:2495–2504, 2013.

[14] Taylor BN, Mehta RR, Yamada T, Lekmine F, Christov K, Chakrabarty AM, Green A, Bratescu L, Shilkaitis A, Beattie C, Das Gupta TK, " Noncationic peptides obtained from Azurin preferentially enter cancer cells," *Cancer Research*. pp. 69:537-546, 2009.

[15] Coelho L, "Anticancer activity of CT-p19LC, a synthetic peptide derived from the bacterial protein azurin," Master of Science Degree dissertation, Scientific Publisher of Lisbon University, 2017.

[16] Huang F, Shu Q, Qin Z, Tian J, Su Z, Huang Y, Gao M, "Anticancer Actions of Azurin and Its Derived Peptide p28," *The Protein Journal* pp. 39:182–189, 2020.

[17] Yamada T, Fialho AM, Punj V, Bratescu L, Gupta TK, Chakrabarty AM, "Internalization of bacterial redox protein azurin in mammalian cells: entry domain and specificity," *Cell Microbiology*, pp. 7:1418–1431, 2005.

[18] Yamada T, Mehta RR, Lekmine F, Christov K, King ML, Majumdar D, Shilkaitis A, Green A, Bratescu L, Beattie CW, Das Gupta TK, "A peptide fragment of azurin induces a p53-mediated cell cycle arrest in human breast cancer cells," *Molecular Cancer Therapeutics*, pp. 8:2947-2958, 2009.

[19] Bernardes N, Garizo AR, Pinto SN, Caniço B, Perdigão C, Fernandes F, Fialho AM, "Azurin interaction with the lipid raft components ganglioside GM-1 and caveolin-1 increases membrane fluidity and sensitivity to anticancer drugs," *Cell Cycle*, pp. 17:13, 1649-1666, 2018.

[20] Gao M, Zhou J, Su Z, Huang Y, "Bacterial cupredoxin azurin hijacks cellular signaling networks: Protein-protein interactions and cancer therapy," *Protein Science*, pp. 26:2334-2341, 2017.

[21] Bernardes N, Chakrabarty AM, Fialho AM, "Engineering of bacterial strains and their products for cancer therapy," *Applied Microbiology Biotechnology,* pp. 97(12):5189-99, 2013.

[22] Fialho AM, Das Gupta TK, Chakrabarty AM, "Designing Promiscuous Drugs? Look at What Nature Made!" *Letters in Drug Design & Discovery*, pp. 4:40-43, 2007.

[23] Yamada T, Goto M, Punj V, Zaborina O, Chen ML, Kimbara K, Majumdar D, Cunningham E, Das Gupta TK, Chakrabarty AM, "Bacterial redox protein azurin, tumor suppressor protein p53, and regression of cancer," *Proc Natl Acad Sci USA*, pp. 99:14098-14103, 2002.

[24] Punj V, Bhattacharyya S, Saint-Dic D, Vasu C, Cunningham EA, Graves J, Yamada T, Constantinou AI, Christov K, White B, Li G, Majumdar D, Chakrabarty AM, Das Gupta TK, "Bacterial cupredoxin azurin as an inducer of apoptosis and regression in human breast cancer," *Oncogene*, pp. 23:2367–2378, 2004.

[25] Yang D, Miao X, Ye Z, Feng J, Xu R, Huang X, Ge F, "Bacterial redox protein azurin induce apoptosis in human osteosarcoma U2OS cells," *Pharmacological Research*, pp. 52:413-421, 2005.

[26] Yamada T, Das Gupta TK, Craig W. Beattie CW, “p28, an Anionic Cell-Penetrating Peptide, Increases the Activity of Wild Type and Mutated p53 without Altering Its Conformation,” *Molecular Pharmaceutics*, pp. 10:3375-3383, 2013.

[27] Himanen, JP, Rajashankar KR, Lackmann M, Cowan CA, Henkemeyer M, Nikolov DB, “Crystal structure of an Eph receptor-ephrin complex,” *Nature*, pp. 414:933-938, 2001.

[28] Chaudhari A, Mahfouz M, Fialho AM, Yamada T, Granja AT, Zhu Y, Hashimoto W, Schlarb-Ridley B, Cho W, Das Gupta TK, Chakrabarty AM, “Cupredoxin-Cancer Interrelationship: Azurin Binding with EphB2, Interference in EphB2 Tyrosine Phosphorylation, and Inhibition of Cancer Growth,” *Biochemistry*, pp. 46:1799-1810, 2007.

[29] Mehta RR, Yamada T, Taylor BN, Christov K, King ML, Majumdar D, Lekmine F, Tiruppathi C, Shilkaitis A, Bratescu L, Gree A, Beattie CW, Das Gupta TK, “A cell penetrating peptide derived from azurin inhibits angiogenesis and tumor growth by inhibiting phosphorylation of VEGFR-2, FAK and Akt,” *Angiogenesis*, pp.14:355–369, 2011.

[30] Ribeiro AS, Albergaria A, Sousa B, Correia AL, Bracke M, Seruca R, Schmitt FC, Paredes J, “Extracellular cleavage and shedding of P-cadherin: a mechanism underlying the invasive behaviour of breast cancer cells,” *Oncogene*, pp. 29:392-402, 2010.

[31] Bernardes N, Ribeiro AS, Abreu S, Mota B, Matos RG, Arraiano CM, Seruca R, Paredes J, Fialho AM, “The Bacterial Protein Azurin Impairs Invasion and FAK/Src Signaling in P-Cadherin-Overexpressing Breast Cancer Cell Models,” *PLoS ONE*, pp. 8(7):e69023, 2013.

[32] Bernardes N, Ribeiro AS, Abreu S, Vieira AF, Carreto L, Santos M, Seruca R, Paredes J, Fialho AM, “High-throughput molecular profiling of a P-cadherin overexpressing breast cancer model reveals new targets for the anti-cancer bacterial protein azurin,” *The International Journal of Biochemistry & Cell Biology*, pp. 50:1-9, 2014.

[33] Bernardes N, Abreu S, Carvalho FA, Fernandes F, Santos NC, Fialho AM, “Modulation of membrane properties of lung cancer cells by azurin enhances the sensitivity to EGFR-targeted therapy and decreased β1 integrin-mediated adhesion,” *Cell Cycle*, pp. 15:1415-1424, 2016.

[34] Yamada T, Das Gupta TK, Craig W. Beattie CW, “p28-Mediated Activation of p53 in G2–M Phase of the Cell Cycle Enhances the Efficacy of DNA Damaging and Antimitotic Chemotherapy,” *Cancer research*, pp. 76:2354-2365, 2016

[35] Choi JH, Lee MH, Cho YJ, Park BS, Kim S, Kim GC, “The Bacterial Protein Azurin Enhances Sensitivity of Oral Squamous Carcinoma Cells to Anticancer Drugs,” Yonsei Medical Journal, pp. 52:773-778, 2011.

[36] Ramachandran S, Mandal M, “Induction of apoptosis of azurin synthesized from *P. aeruginosa* MTCC 2453 against Dalton’s lymphoma ascites model,” *Biomedicine & Pharmacotherapy,* pp. 65:461-466, 2011.

[37] Abuei H, Behzad-Behbahani A, Faghihi F, Farhadi A, Dehbidi GRR, Pirouzfar M, Zare F, "The Effect of Bacterial Peptide p28 on Viability and Apoptosis Status of P53-null HeLa Cells," *Advanced Pharmaceutical Bulletin*, Vol. 9, pp. 4:668-673, 2019.

[38] Ghasemi-Dehkordi P, Doosti A, Jami M, "The concurrent effects of azurin and Mammaglobin-A genes in inhibition of breast cancer progression and immune system stimulation in cancerous BALB/c mice," *3 Biotech*, pp. 9:271-285, 2019.

[39] Shahbazi S, Bolhassani A, "Comparison of six cell penetrating peptides with different properties for in vitro and in vivo delivery of HPV16 E7 antigen in therapeutic vaccines," *International Immunopharmacology*, pp. 62:170–180, 2018

[40] Zhang Y, Zhang Y, Xia L, Zhang X, Ding X, Yan F, Wu F, "*Escherichia coli* Nissle 1917 Targets and Restrains Mouse B16 Melanoma and 4T1 Breast Tumors through Expression of Azurin Protein," *Applied and Environmental Microbiology*, pp. 78:7603–7610, 2012.

[41] Mehta N, Lyon JG, Patil K, Mokarram N, Kim C, Bellamkonda RV, "Bacterial Carriers for Glioblastoma Therapy," *Molecular Therapy: Oncolytics*, pp. 4:1-17, 2017.

[42] Soleimania M, Sadeghib HM, Jahanian-Najafabadi A, "A Bi-Functional Targeted P28-NRC Chimeric Protein with Enhanced Cytotoxic Effects on Breast Cancer Cell Lines," *Iranian Journal of Pharmaceutical Research*, pp. 18: 735-744, 2018.

[43] Micewicz ED, Chun-Ling J, Schaue D, Luong H, McBride WH, Ruchala P, "Small azurin derived peptide targets ephrin receptors for radiotherapy," *International Journal of Peptide Research and Therapeutics*, pp. 17:247-257, 2011.

[44] Paydarnia N, Khoshtinat Nikkhoi S, Fakhravar A, Mehdiabdol M, Heydarzadeh H, Ranjbar S, "Synergistic effect of granzyme B-azurin fusion protein on breast cancer cells," *Molecular Biology Reports*, pp. 46:3129-3140, 2019.

[45] Warso MA, Richards JM, Mehta D, Christov K, Schaeffer C, Bressler LR, Yamada T, Majumdar D, Kennedy SA, Beattie CW, Das Gupta TK, "A first-in-class, first-in-human, phase I trial of p28, a non-HDM2-mediated peptide inhibitor of p53 ubiquitination in patients with advanced solid tumours," *British Journal of Cancer*, pp. 108: 1061–1070, 2013.

[46] Lulla RR, Goldman S, Yamada T, Beattie CW, Bressler L, Pacini M, Pollack IF, Fisher PG, Packer RJ, Dunkel IJ, Dhall G, Wu S, Onar A, Boyett JM, Foulad M, "Phase 1 trial of p28 (NSC745104), a non-HDM2-mediated peptide inhibitor of p53 ubiquitination in pediatric patients with recurrent or progressive central nervous system tumors: A Pediatric Brain Tumor Consortium Study," *Neuro-Oncology*, pp. 18:1319-1325, 2016.

[47] Gajate C, Santos-Beneit AM, Macho A, Lazaro MC, Hernandez-De Rojas A, Modolell M, Muñoz E, Mollinedo F, "Involvement of mitochondria and caspase-3 in ET-18-OCH_3-induced apoptosis of human leukemic cells," *International Journal of Cancer*, pp. 86:208-218, 2000.

[48] Rienzo FD, Gabdoulline RR, Menziani MC, Wade RC, “Blue copper proteins: a comparative analysisof their molecular interaction properties,” *Protein Science*, pp. 9:1439–1454, 2000.

[49] Murphy LM, Dodd FE, Yousafzai FK, Eady RR, Hasnain SS, “Electron donation between copper containing nitrite reductases and cupredoxins: the nature of protein–protein interaction in complex formation,” *Journal of Molecular Biology*, pp. 315:859–871, 2002.

[50] Hanahan D, Weinberg RA, “Hallmarks of cancer: The next generation,” Cell, pp 144:646–674, 2011.

[51] Burgermeister E, Xing X, Röcken C, Juhasz M, Chen J, Hiber M, Mair K, Shatz M, Liscovitch M, Schmid RM, Ebert MPA, “Differential Expression and Function of Caveolin-1 in Human Gastric Cancer Progression,” Cancer Res., pp. 67:8519-85, 2007.

[52] Raguz S, Yagüe E, “Resistance to chemotherapy: New treatments and novel insights into an old problem,” Br. J. Cancer, pp. 99:387–391, 2008.

[53] Karpiński TM, Adamczak A, “Anticancer Activity of Bacterial Proteins and Peptides,” Pharmaceutics, Vol. 10, no. 2: 54, 2018.

[54] Wolf P, Elsasser-Beile U, “Pseudomonas exotoxin A-based immunotoxins for targeted cancer therapy,” In: Emerging cancer therapy: Microbial approaches and biotechnological tools, Fialho AM, Chakrabarty AM (eds), John Wiley and Sons, 2010.

[55] Murphy JR, “Mechanism of diphtheria toxin catalytic domain delivery to the eukaryotic cell cytosol and the cellular factors that directly participate in the process,” Toxins (Basel), pp. 3:294-308, 2011.

[56] Lutz MB, Baur AS, Schuler-Thurner B, Schuler G, “Immunogenic and tolerogenic effects of the chimeric IL-2-diphtheria toxin cytocidal agent Ontak® on CD25+ cells,”, Oncoimmunology, 3, e28223, 2014.

[57] Lee, D.G.; Hahm, K.-S.; Park, Y.; Kim, H.Y.; Lee, W.; Lim, S.C.; Seo, Y.K.; Choi, C.H. Functional and structural characteristics of anticancer peptide Pep27 analogues. Cancer Cell Int. 2005, 5, 21.

[58] Giansanti F, Panella G, Leboffe L, Antonini G, “Lactoferrin from Milk: Nutraceutical and Pharmacological Properties,” Pharmaceuticals, Vol. 9, no. 4: 61, 2016.

[59] Zhang Y, Lima CF, Rodrigues LR, “Anticancer effects of lactoferrin: underlying mechanisms and future trends in cancer therapy,” Nutrition Reviews, Vol. 72, pp. 12:763–773, 2014.

[60] Pan WR, Chen PW, Chen YLS, Hsu HC, Lin CC, Chen WJ, “Bovine lactoferricin B induces apoptosis of human gastric cancer cell line AGS by inhibition of autophagy at a late stage,” Volume 96, pp. 12:7511-7520, 2013.

[61] Fang B, Guo HY, Zhang, M, Jiang, L, Ren FZ, “The six amino acid antimicrobial peptide bLFcin6 penetrates cells and delivers siRNA,” FEBS J. pp. 280:1007–1017, 2013.